Humanities & Social Sciences Communications

ARTICLE

https://doi.org/10.1057/s41599-025-06212-w OPEN

Check for updates

Tailoring tail risk models for clean energy investments: a dual approach to long and short position forecasting

Wei Kuang[1,2] ✉

The increasing focus on sustainable finance has highlighted the critical need for accurate risk assessment in clean energy investments. However, existing research often overlooks the sector's distinctive volatility characteristics, resulting in ineffective risk management approaches that fail to distinguish between the varied risk profiles associated with long and short positions in clean energy equities. This study addresses this gap by improving the forecasting accuracy of tail risk assessments through novel adaptations of existing volatility modeling frameworks. We demonstrate that different modeling paradigms, which assume different statistical properties for price volatility and return distributions, are required for accurate forecasting of long and short positions. Specifically, models incorporating asymmetric volatility responses and heavy-tailed distributions excel for long holdings, while models allowing for highly persistent volatility effects combined with skewed distributions perform best for short positions. This differentiated approach reflects the intrinsic asymmetries in clean energy markets. Our rigorous empirical investigation, spanning more than a decade and including severe market upheavals, reveals that these tailored models significantly outperform standard methods. The findings provide practical insights for investors and regulators by demonstrating how targeted modeling methodologies can effectively capture the complex dynamics of clean energy investments, thus supporting the broader goals of sustainable finance.

[1] School of Sport Business, Guangzhou Sport University, Guangzhou, China. [2] Guangdong Provincial Key Laboratory of Human Sports Performance Science, Guangzhou Sport University, Guangzhou, China. ✉email: kuangwei8355@hotmail.com

Introduction

The renewable energy sector has grown dramatically over the last decade, accompanied by increased market capitalization and investment flows. The "Energy Transition Investment Trends 2024" report by BloombergNEF indicates a 17% rise in global investments in the low-carbon energy transition in 2023, totaling around $1.77 trillion (BloombergNEF, 2024). In tandem, the International Energy Agency's (IEA) "Renewables 2023" publication reveals a nearly 50% increase in global annual renewable capacity additions, reaching a record 510 gigawatts (IEA, 2023). This is the fastest growth rate in two decades and the 22nd consecutive year of record-setting additions (IEA, 2023). These trends highlight the sector's resiliency and critical role in promoting economic growth and innovation to ensure a sustainable future. According to the IEA, while the world is on track to more than double renewable energy capacity by 2030, further support is required to meet the net-zero emissions objective by mid-century (IEA, 2024).

Despite this expansion, the clean energy stock markets have experienced increased volatility and risk, with sharp price fluctuations and market corrections. The sector experienced substantial declines in the early phases of the COVID-19 pandemic in 2020 (Liu et al., 2022), as global markets responded to economic instability. The sector's fast rebound, fueled by investor expectations of a green shift in global energy regulations, was followed by further volatility into 2021 (NS Energy, 2021). For example, the WilderHill Clean Energy Index (ECO), which tracks the performance of companies in the renewable energy and conservation sectors, has undergone major corrections after reaching record highs (WilderShares LLC, 2022a). This volatility continued into 2022, influenced by market forces such as supply-chain issues, inflation concerns, and geopolitical tensions (WilderShares LLC, 2022b). The persistent volatility highlights the importance of investors using accurate risk assessment and management tools to efficiently navigate the complexity of the clean energy market.

The burgeoning field of clean energy equities has garnered substantial scholarly attention, particularly in relation to traditional energy and financial assets like oil and technology stocks. Existing literature extensively examines mean returns, volatility, tail risk spillovers, and price forecasting in this domain (e.g., Dutta et al., 2020a; Inchauspe et al., 2015; Managi and Okimoto, 2013; Reboredo et al., 2017; Sadorsky, 2012a, 2022; Saeed et al., 2021). However, despite the high-risk profile associated with clean energy investments (e.g., Ortas and Moneva, 2013; Rezec and Scholtens, 2017), there remains a critical shortcoming in the literature regarding effective risk management strategies, particularly concerning hedging techniques and volatility risk mitigation (e.g., Ahmad et al., 2018; Gustafsson et al., 2022). Notably, the prediction of tail risks in clean energy equities has been under-explored, with limited examination of how distributional features and volatility dynamics affect forecasting accuracy (Pradhan and Tiwari, 2021; Zhuo et al., 2023). Furthermore, prior research has not rigorously investigated the performance of predictive models across different investment strategies specifically distinguishing between long and short positions, nor has it compared the efficacy of various tail risk models like Value at Risk (VaR) and Expected Shortfall (ES).

These research gaps are particularly significant because modeling tail risk during market stress remains a major challenge in financial econometrics. The 2008 financial crisis exposed the limitations of standard VaR models and prompted extensive research into more robust approaches (Berger and Missong, 2014; Chen et al., 2012), including comparative studies aimed at identifying optimal VaR specifications for turbulent periods (Abad et al., 2016; Louzis et al., 2014; Tran and Tran, 2023). Notably, Halbleib and Pohlmeier (2012) showed that, although individual VaR models often failed during crises, their performance could be improved through data-driven forecast combination techniques, highlighting the importance of addressing model misspecification risk. Rather than proposing new methodologies, this study contributes to the literature by systematically applying established models to clean energy assets, an area still underexplored in risk modeling. Specifically, we investigate whether carefully tailoring model specifications for long and short positions can serve as an alternative path to improving VaR forecasts, parallel to the improvements achieved by combination methods in the existing VaR literature (Chiu et al., 2010; Taylor, 2020). In doing so, we extend robust post-crisis frameworks to address the unique risks of clean energy investments.

Addressing these deficiencies is crucial for several interconnected reasons. As the clean energy sector experiences unprecedented growth and attracts significant investment flows, accurate risk assessment and management have become increasingly vital (Demiralay et al., 2023). The absence of robust, sector-specific risk models creates fundamental vulnerabilities whereby investors systematically underestimate potential losses, resulting in suboptimal capital allocation that hinders sectoral development. This concern becomes particularly acute for tail risk, i.e. the probability of rare but severe, high-impact events. Empirical evidence demonstrates that clean energy asset returns exhibit pronounced "fat tails" and negative skewness, indicating that extreme losses occur with significantly greater frequency than predicted by standard normal distributions (Zhang et al., 2023a). Traditional risk frameworks that assume normality systematically underestimate both the probability and magnitude of worst-case scenarios, exposing investors to substantial downside risk (Sheikh and Qiao, 2010). Consequently, developing models capable of capturing these non-normal characteristics represents a central methodological challenge, particularly as regulatory frameworks evolve to support sustainable investments, creating urgent demand for sophisticated risk measures in this inherently volatile sector.

The asymmetric nature of volatility in clean energy markets further compounds these modeling challenges and necessitates increasingly nuanced analytical approaches (Zhang et al., 2023). Financial markets exhibit a well-documented phenomenon whereby negative news generates disproportionately larger increases in future volatility compared to positive news of equivalent magnitude-a relationship known as the leverage effect (Black, 1976). This asymmetric volatility response proves particularly pronounced within the clean energy sector, which demonstrates heightened sensitivity to adverse regulatory announcements, supply chain disruptions, and technological failures (Hassan, 2023; Zhao, 2020). Risk models that fail to incorporate this asymmetric behavior will systematically miscalculate volatility escalation following negative market events, thereby leaving long-position investors inadequately prepared for subsequent market turbulence. These empirical realities provide direct motivation for employing asymmetric volatility models specifically designed to capture leverage effects (Engle and Ng, 1993).

The distinction between long and short position risk profiles represents another critical dimension that has received insufficient attention in existing literature. Long positions, predominantly held by institutional investors optimistic about clean energy prospects, require protection against sudden market downturns. Conversely, short positions, employed by hedge funds and risk managers for speculative or hedging purposes, face qualitatively different exposures, including potential unlimited losses during rapid price appreciation. Despite these divergent risk characteristics, the majority of financial risk literature maintains an implicit long-only focus, concentrating on modeling downside movements while leaving short position dynamics under-explored. This constitutes a critical gap, as models optimized for downside risk may prove ill-suited for quantifying upside risk exposures (Angelidis and Degiannakis, 2005). The present research addresses this limitation by proposing a dual-risk framework that independently assesses model performance for both strategies, providing market participants with a more complete and practically relevant risk management toolkit.

Overall, this study fills these significant gaps by making the following three innovative contributions:

First, we introduce and validate a dual-risk framework for the clean energy sector. To our knowledge, this is the first study to systematically model and backtest tail risk for both long and short positions in clean energy equities. By demonstrating that optimal risk models differ significantly between these two strategies, we challenge the conventional one-size-fits-all approach and provide more targeted, practical insights for a wider range of market participants, from long-term investors to hedge funds.

Second, we improve the methodology of risk modeling by tailoring volatility models to the unique characteristics of clean energy stocks. We refine a set of established conditional volatility models chosen to represent symmetric, asymmetric, and highly persistent volatility structures, by integrating sophisticated distributional assumptions that more accurately capture the observed skewness and fat tails in clean energy returns. This methodological enhancement increases the predictive power of these models for this specific, under-researched asset class.

Third, we provide robust empirical validation across multiple market regimes. Our analysis is not limited to a single market environment but draws on over a decade of data, including major market upheavals like the 2008 financial crisis and the COVID-19 pandemic. By rigorously backtesting our models through these periods of extreme stress, we offer strong evidence of their reliability and real-world applicability, providing actionable insights for investors, risk managers, and policymakers navigating this volatile sector.

The remainder of the article is organized as follows. Section 2 provides a literature review. Section 3 outlines the models and evaluation methods. Section 4 explains the data and presents the empirical findings. Section 5 concludes.

Literature review

The intricate interdependencies between clean energy stock prices and other financial assets are pivotal to understanding their risk profiles. Pioneering work in this domain reveals that renewable energy equities are significantly influenced by technology shares and oil prices, suggesting a unidirectional impact (Henriques and Sadorsky, 2008). Kumar et al. (2012) substantiates this by revealing a stronger linkage with technology equities over oil prices. The 2008 financial crisis exacerbated the correlation between oil prices and the valuation of renewable and technology companies (Sadorsky, 2012a). This trend continued, with Inchauspe et al. (2015) observing a significant influence of the MSCI World index and technology shares on renewable energy investments post-2007, albeit with an increasing influence of oil prices. In contrast, Dutta et al. (2020a) emphasizes an increased sensitivity of green investments to oil market volatility rather than price fluctuations. Moreover, leveraging advanced machine learning techniques, Sadorsky (2022) has identified technical indicators and market volatility measures as key predictors of clean energy stock prices, highlighting the nuanced relationships these stocks have with technology and oil assets.

The second strand of literature examines extreme risk spillovers in the renewable energy sector. Tan et al. (2021) uses a spillover index and multivariate quantile models to uncover asymmetric and time-varying risk relationships between oil and clean energy equities, identifying the oil market as a net recipient of volatility. Zhang et al. (2023) builds on volatility models that link short-term market risk to long-term macroeconomic trends, emphasizing the importance of asymmetric market reactions and extreme events. Studies by Di Febo et al. (2021) and Saeed et al. (2021) contribute to the discussion of tail risk dynamics, highlighting the significance of considering market asymmetry during times of stress. Other researchers such as Hassan (2023), Xia et al. (2019), and Fu et al. (2022) investigated how external factors like energy security and macroeconomic indicators affect the volatility of clean energy stock during volatile market periods. Naeem and Arfaoui (2023) and Syuhada et al. (2024) used conditional risk models to explore systemic risk and interconnectedness in energy markets, while Zhang et al. (2023b) and Chen et al. (2022) found increased interconnectedness during extreme market conditions.

From a risk management perspective, the high volatility of renewable energy stocks has attracted considerable academic interest. Sadorsky (2012b) and Ortas and Moneva (2013) examined the key risk drivers for renewable energy companies, with Ortas and Moneva (2013) identifying a structural shift in risk levels during the financial crisis. More recently, Lehnert (2023) and Ghosh et al. (2022) have drawn parallels with historical market bubbles, suggesting that clean energy stocks may be subject to similar market dynamics. From a hedging viewpoint, Ahmad et al. (2018) and Gustafsson et al. (2022) investigated optimal hedges for clean energy stocks, with the latter finding that traditional energy metals are not effective hedges for clean energy equities. Moreover, Troster et al. (2020), Pradhan and Tiwari (2021) and Zhuo et al. (2023) have made notable contributions by using the VaR or ES techniques to assess market risk, with the research by Zhuo et al. (2023) highlighting the superior performance of conditional volatility models, particularly during the COVID-19 pandemic. Despite the extensive research, gaps remain. The analysis by Troster et al. (2020), Pradhan and Tiwari (2021) and Zhuo et al. (2023) focused on long positions while ignoring the impact of short positions on risk modeling. The reliance on traditional conditional volatility models by Pradhan and Tiwari (2021) and Zhuo et al. (2023) fails to account for critical volatility aspects such as leverage effect and long memory, which are necessary for accurate tail risk forecasting. Furthermore, these studies lack a comparative study across different market stress levels, as well as direct comparisons between VaR and ES projections, both of which are crucial for determining the relative usefulness of these risk measures. This research gap serves as the foundation for our investigations.

Methods and models

Value at Risk (VaR) serves as a pivotal risk metric mandated by the Basel Committee on Banking Supervision (BCBS) in 1996 for quantifying the potential maximum loss a financial portfolio may incur over a specified time horizon, typically one day, at a chosen confidence level. The formula for VaR at a confidence level $(1-\alpha)$ is $\Pr\left(r_{t+h} \leq \mathrm{VaR}_{t+h}^{\alpha}\right) = \alpha$ where r_{t+h} denotes the return of the portfolio at time $t+h$. Expected Shortfall (ES), also known as Conditional VaR, extends the VaR concept by not only quantifying the potential loss but also providing the expected size of loss given that the VaR threshold has been breached. The BCBS has recommended a shift in the regulatory framework from using a 99% confidence level VaR to a 97.5% confidence level ES for a more nuanced quantification of risk BCBS (2016) .

The logarithmic daily return of a financial asset, denoted by r_t, is modeled as follows:

$$r_t = \mu_t + \varepsilon_t = (c_0 + c_1 r_{t-1}) + \varepsilon_t \tag{1}$$

$$\varepsilon_t = \sigma_t z_t \tag{2}$$

Here, the conditional mean, μ_t, is modeled as a first-order autoregressive AR(1) process to account for any serial correlation in the returns (Troster et al., 2020). In this mean equation, c_0 represents the constant term (intercept), and c_1 is the autoregressive coefficient that captures the effect of the previous day's return r_{t-1} on the current day's return. The term ε_t is the residual at time t, which is composed of the conditional volatility, σ_t, and an independent and identically distributed (i.i.d.) random variable, z_t, with a mean of zero and variance of one.

For the purpose of one-day ahead risk assessment, the VaR and ES are estimated using the following expressions (Brio et al., 2020):

$$\mathrm{VaR}_t^{\alpha} = \hat{\mu}_t + \hat{\sigma}_t \hat{F}_z^{-1}(\alpha) \tag{3}$$

$$\mathrm{ES}_t^{\alpha} = \hat{\mu}_t + \hat{\sigma}_t \hat{S}_z(\alpha) \tag{4}$$

Here, $\hat{\mu}_t$ and $\hat{\sigma}_t$ represent the predicted values for the daily conditional mean and conditional volatility, respectively. $\hat{F}_z^{-1}(\alpha)$ signifies the inverse cumulative distribution function (CDF) of the standardized innovations at the α quantile, and $\hat{S}_z(\alpha)$ represents the expected value of z given that z is less than its α quantile.

As demonstrated by Equations (3) and (4), the accuracy of one-day-ahead VaR and ES forecasts depends critically on the precise estimation of two key components: the conditional volatility σ_t and the quantile of the standardized innovations $F_z^{-1}(\alpha)$. The volatility forecast scales the overall risk estimate, capturing the time-varying magnitude of market fluctuations, while the innovation distribution determines the shape of the tail risk, particularly in extreme market conditions. Inaccurate volatility modeling leads to risk estimates that are consistently biased, while incorrect distributional assumptions result in fundamental miscalculations of tail probabilities. The following subsections detail the specific models used to estimate these two primary drivers of tail risk.

Volatility models. A core feature of financial returns is the phenomenon of volatility clustering, where periods of high volatility tend to be followed by more high volatility, and calm periods are followed by calm periods (Engle, 1982). The Generalized Autoregressive Conditional Heteroskedasticity (GARCH) family of models is specifically designed to capture this time-varying nature of financial risk (Bollerslev, 1986).

The decision to utilize GARCH-type models for volatility analysis in clean energy stocks is anchored in both theoretical and empirical considerations. They are widely recognized for their ability to capture stylized facts of financial time series, such as volatility clustering and leptokurtosis (Bollerslev, 1986; Engle, 1982). These features are particularly pertinent in the clean energy sector, where returns are often characterized by rapid technological change, policy uncertainty, and shifting investor sentiment (Athari and Kirikkaleli, 2025; Song et al., 2019). Moreover, GARCH models offer a practical balance between flexibility and parsimony, delivering reliable performance while remaining computationally efficient and interpretable for practitioners (Francq and Zakoian, 2019). This transparency and theoretical foundation are crucial for risk management, particularly when compared to advanced machine learning techniques, which often function as "black boxes" with high data requirements and increased risk of overfitting (Alessi and Savona, 2021; Wang, 2024). Given their extensive validation and widespread adoption, GARCH-type models provide a robust and comparable framework for our analysis (Christoffersen, 2012).

In this study, we employ three distinct GARCH specifications to test competing hypotheses about the volatility dynamics characterizing clean energy stocks. The standard GARCH model (Bollerslev, 1986) serves as our foundational benchmark, assuming symmetric volatility responses. To test for the leverage effect, we employ the Glosten, Jagannathan, and Runkle (GJR) GARCH specification (Glosten et al., 1993), which allows for asymmetric volatility responses to positive and negative news. Additionally, to investigate whether volatility shocks exhibit exceptional persistence, we use the Integrated GARCH (IGARCH) model (Engle and Bollerslev, 1986), which allows for near-permanent effects of market disturbances. The specific mathematical formulations for each model are detailed in the following subsections.

Standard GARCH. The GARCH model, introduced by Bollerslev (1986), is a widely used framework for modelling volatility in financial time series. The GARCH(1,1) model, in particular, is characterized by its ability to capture phenomenon of volatility clustering, where large changes in asset prices are often followed by further large changes, and periods of small price changes are followed by further small changes. The GARCH(1,1) model for the conditional variance of a time series r_t is given by:

$$\sigma_t^2 = \omega + \alpha\varepsilon_{t-1}^2 + \beta\sigma_{t-1}^2 \tag{5}$$

Where ω is a constant term, and α and β are parameters to be estimated, with $\alpha + \beta < 1$, ensuring that the conditional variance σ_t^2 remains positive and stationary. The persistence of volatility is captured by the sum of α and β. Specifically, as the sum $\alpha + \beta$ approaches 1, the decay rate of the autocorrelation associated with the conditional variance σ_t decreases toward zero. This implies that shocks to volatility have an increasingly persistent effect.

GJRGARCH. The GJRGARCH model is an extension of the standard GARCH model that allows for asymmetric effects of past shocks on volatility (Glosten et al., 1993). This model is particularly useful when the impact of negative and positive shocks on future volatility is different, a feature known as the leverage effect. This asymmetry is particularly relevant for clean energy equities, which are highly susceptible to regulatory announcements and technological developments (Li, 2023; Zhao et al., 2018). The GJRGARCH(1,1) model is specified as follows:

$$\sigma_t^2 = \omega + [\alpha + \gamma I(\varepsilon_{t-1} < 0)]\varepsilon_{t-1}^2 + \beta\sigma_{t-1}^2 \tag{6}$$

where $I(\cdot)$ is an indicator function that takes the value of 1 if $\varepsilon_{t-1} < 0$ and 0 otherwise, and γ captures the additional impact of negative shocks on future volatility. If $\gamma > 0$, negative shocks increase volatility more than positive shocks.

IGARCH. The IGARCH model (Engle and Bollerslev, 1986) is a special case of the GARCH(1,1) model in which the sum of α and β is constrained to equal one, implying a unit root in the GARCH process and thus persistence of shocks to the variance over an infinite horizon. This specification is well-suited for clean energy markets, which often experience protracted periods of heightened volatility during policy debates and technology development cycles (Athari and Kirikkaleli, 2025). The IGARCH(1,1) model is specified as follows:

$$\sigma_t^2 = \omega + \alpha\varepsilon_{t-1}^2 + \beta\sigma_{t-1}^2 \tag{7}$$

where $\alpha + \beta = 1$. This specification suggests that shocks to the conditional variance have a persistent effect on future volatility levels.

Innovation models. After accounting for time-varying volatility with a GARCH model, the remaining standardized residuals (z_t in Equation (2)) are known as innovations. The distributional assumption made about these innovations is critical for accurately forecasting tail risks like VaR and ES. Although GARCH-type models with normal innovations can generate data with unconditionally fat tails, they are insufficient to account for all of the unconditional leptokurtosis and skewness observed in financial return series (Kuang, 2021). This is particularly important for clean energy markets, which are often subject to extreme events such as sudden price jumps or collapses driven by policy changes and technological breakthroughs.

To address this empirical reality, our study follow Kuang (2022) to evaluates four distinct innovation distributions, each representing a different approach to capturing the true characteristics of clean energy stock returns: The Normal distribution serves as the conventional benchmark, despite its likely misspecification for financial data. The skewed Student's t-distribution provides a flexible parametric framework to simultaneously capture both asymmetry and heavy tails Fernandez and Steel (1998). The Filtered Historical Simulation (FHS) offers a non-parametric alternative that makes no distributional assumptions, instead utilizing the empirical distribution of historical innovations directly Barone-Adesi et al. (1999). The Cornish-Fisher expansion represents a semi-parametric compromise, adjusting normal distribution quantiles based on the observed higher-order moments of the innovation series Favre and Galeano (2002). The mathematical specifications and risk forecasting equations for each approach are detailed in the subsequent subsections.

Normal distribution. The normal distribution assumption is both the simplest and the most commonly used for financial return innovations, mainly because of its analytical convenience. Assuming that the standardized residual z_t adheres to a standard normal distribution, its cumulative distribution function delineated as follows:

$$\Phi(x) = \frac{1}{\sqrt{2\pi}}\int_{-\infty}^{x} e^{-t^2/2} \tag{8}$$

The next days' risk forecasts are provided as below (Brio et al., 2020):

$$\mathrm{VaR}_{t,N}^{\alpha} = \hat{\mu}_t + \hat{\sigma}_t\Phi^{-1}(\alpha) \tag{9}$$

$$\mathrm{ES}_{t,N}^{\alpha} = \hat{\mu}_t + \hat{\sigma}_t\frac{1}{\alpha}\phi\left[\Phi^{-1}(\alpha)\right] \tag{10}$$

In this context, ϕ represents the probability density function (pdf) of a standard normal distribution, while $\Phi^{-1}(\alpha)$ denotes the corresponding quantile for an arbitrary value of α.

Skewed student distribution. The skewed Student's t-distribution, as proposed by Fernandez and Steel (1998), accommodates both skewness and excess kurtosis in the distribution of innovations. The quantile function for the skewed Student's t-distribution can be written as below (Lambert and Laurent, 2001):

$$c_{\alpha,\nu,\xi}^{skst} = \begin{cases} \left\{\frac{1}{\xi}c_{\alpha,\nu}^{st}\left[\frac{\alpha}{2}\left(1+\xi^2\right)\right] - m\right\}/s, & \text{if } \alpha < \frac{1}{1+\xi^2} \\ \left\{-\xi c_{\alpha,\nu}^{st}\left[\frac{1-\alpha}{2}\left(1+\xi^{-2}\right)\right] - m\right\}/s, & \text{if } \alpha \geq \frac{1}{1+\xi^2} \end{cases} \tag{11}$$

where $c_{\alpha,\nu,\xi}^{skst}$ represents the αth quantile of the skewed student distribution with unit variance, characterized by $\nu > 2$ degrees of freedom and an asymmetric parameter $\xi > 0$. The term $c_{\alpha,\nu}^{st}$ denotes the quantile function of the standardized Student-t density function. In addition, m and s stand for the non-standardized skewed student distribution's mean and standard deviation, respectively. Consequently, the next days' risk forecasts are provided as follows:

$$\mathrm{VaR}_{t,skst}^{\alpha} = \hat{\mu}_t + \hat{\sigma}_t c_{\alpha,\nu,\xi}^{skst} \tag{12}$$

$$\mathrm{ES}_{t,skst}^{\alpha} = \hat{\mu}_t + \hat{\sigma}_t\mathbb{E}\left[z|z < c_{\alpha,\nu,\xi}^{skst}\right] \tag{13}$$

Filtered historical simulation. The Filtered Historical Simulation (FHS) method is a semi-parametric technique Barone-Adesi et al. (1999). This approach uses a non-parametric estimator for the residual distribution and parametric models for the mean and volatility dynamics. Subsequently, the next days' risk forecasts are provided as follows:

$$\mathrm{VaR}_{t,HS}^{\alpha} = \hat{\mu}_t + \hat{\sigma}_t\hat{H}^{-1}(\alpha) \tag{14}$$

$$\mathrm{ES}_{t,HS}^{\alpha} = \hat{\mu}_t + \hat{\sigma}_t\mathbb{E}\left[z|z < \hat{H}^{-1}(\alpha)\right] \tag{15}$$

where the α quantile of the empirical distribution of the standardized residual z_t is indicated by $\hat{H}^{-1}(\alpha)$.

Cornish-Fisher expansion. The Cornish-Fisher expansion, as proposed by Favre and Galeano (2002), is a semi-parametric method that modifies the quantiles of a normal distribution to incorporate skewness and kurtosis. The α quantile of a distribution is defined as below.

$$\delta_{\mathrm{CF}}(\alpha) = Z(\alpha) + \frac{1}{6}\left(Z(\alpha)^2 - 1\right)S + \frac{1}{24}\left(Z(\alpha)^3 - 3Z(\alpha)\right)K - \frac{1}{36}\left(2Z(\alpha)^3 - 5Z(\alpha)\right)S^2 \tag{16}$$

where $Z(\alpha)$ represents the standard normal distribution's α quantile. Additionally, S and K symbolize the innovation distribution's excess kurtosis and skewness, respectively. The risk forecasts for the upcoming day are shown below:

$$\mathrm{VaR}_{t,CF}^{\alpha} = \mu_t + \hat{\sigma}_t\delta_{\mathrm{CF}}(\alpha) \tag{17}$$

$$\mathrm{ES}_{t,CF}^{\alpha} = \hat{\mu}_t + \hat{\sigma}_t\mathbb{E}\left[z|z < \delta_{\mathrm{CF}}(\alpha)\right] \tag{18}$$

Backtesting. This study adheres to the analytical framework of Kuang (2022) by employing a dual approach to backtesting methods. We integrate conventional VaR backtesting techniques with advanced ES backtesting methods, which provide a more nuanced evaluation of model performance in capturing tail risk. This comprehensive approach is further complemented by the evaluation of loss functions, which serve as a quantitative measure to compare the relative efficacy of various forecasting models. By using these robust methodologies, our analysis aims to provide a rigorous assessment of the predictive capabilities of models, ensuring a more accurate and reliable risk management strategy for investors and practitioners in the clean energy sector.

Value-at-risk. The Actual over Expected (AE) Exceedance Ratio is a simple backtesting metric that compares the number of exceedances to the expected number under the null hypothesis of model adequacy. A ratio close to one indicates a well-calibrated model, while a ratio significantly above or below than one suggests over- or underestimation of risk by the model, respectively. More strict backtesting procedures are based on the statistical tests described below.

The Unconditional Coverage Test, denoted as LR_{uc} by Kupiec (1995), evaluates the congruence of exceedance proportions with anticipated levels over a specified time frame. This test assumes that exceedances are independently and identically distributed, an assumption that is often not met in financial returns. Under the null hypothesis that the model provides correct unconditional coverage, the LR_{uc} test statistic is asymptotically distributed as a chi-squared $\left(\chi^2\right)$ variable with one degree of freedom.

The Conditional Coverage Test, proposed by Christoffersen (1998) and referred to as LR_{cc}, combines the Unconditional Coverage Test with a test for exceedance independence. This provides a joint test statistic capable of identifying both correct coverage and temporal independence of exceedances. The resulting LR_{cc} test statistic follows an asymptotic chi-squared (χ^2) distribution with two degrees of freedom under the null hypothesis of correct conditional coverage.

Finally, the Dynamic Quantile (DQ) test, introduced by Engle and Manganelli (2004), uses a regression-based methodology to assess whether VaR exceedances can be predicted on the basis of their previous values or other data points. This provides a direct assessment of correct conditional coverage and is adept at incorporating dynamic elements into quantile predictions. The DQ test statistic is also asymptotically distributed as a chi-squared (χ^2) variable, with the degrees of freedom equal to the number of included lags and other explanatory variables in the test regression (excluding the intercept).

Expected shortfall. The Exceedance Residuals (ER) test, as introduced by McNeil and Frey (2000), serves as a prevalent method for evaluating ES models. This test quantifies the ER as the difference between the actual return and the ES forecast when a VaR breach occurs. The ER test operates under the premise that a well-calibrated risk model should result in an ER with an expected value of zero. To validate this, the bootstrap method, pioneered by Efron and Tibshirani (1993), is utilized. This method employs a one-tailed test to assess whether a negative mean ER suggests a systematic bias in the ES forecasts, indicating that the model consistently underestimates the ES.

The ES regression (ESR) test, proposed by Bayer and Dimitriadis (2022), approaches the evaluation of ES forecasts by treating the conditional ES as a linear function of returns. In this framework, returns are the dependent variable, and the ES forecasts, which include an intercept term, are the independent variables. For accurate specification of ES forecasts, the intercept and slope parameters should ideally be zero and one, respectively. To further refine the assessment, Bayer and Dimitriadis (2022) recommend an Intercept ESR test. This test focuses on the intercept term, ensuring that the ES forecasts are not consistently biased low. By constraining the slope parameter to one, the method isolates the intercept for evaluation, providing a targeted test for the accuracy of ES predictions.

MCS tests. The Model Confidence Set (MCS) approach, as developed by Hansen et al. (2011), is employed in this study to evaluate and compare the performance of various forecasting models. The MCS method is a statistical tool designed to identify a subset of models that outperform others at a specified confidence level. In this research, MCS testing is conducted at a 90% confidence level, utilizing different loss functions to assess the predictive accuracy of risk forecasts. Models that exhibit lower average loss levels over the projection period are deemed to have superior performance, providing a more nuanced evaluation than individual statistical tests.

The Quasi-Likelihood (QLIKE) loss function is utilized to evaluate the accuracy of volatility predictions, with daily squared returns serving as a surrogate for realized volatility (RV). The QLIKE function is asymmetric, penalizing under-forecasting more severely than over-forecasting. This property, along with its robustness against noise in the volatility proxy, as demonstrated by Patton (2011), makes it a preferred choice over the Mean Squared Error (MSE) for assessing volatility forecasts. The QLIKE function's reduced sensitivity to outliers further enhances its suitability for evaluating volatility models. The QLIKE function is defined as:

$$\mathrm{QLIKE}_t = \frac{\mathrm{RV}_t}{\hat{\sigma}_t^2} - \ln\left(\frac{\mathrm{RV}_t}{\hat{\sigma}_t^2}\right) - 1 \tag{19}$$

In the context of quantile forecast evaluation, the Tick Loss Function (TLF) is employed. This technique, derived from quantile regression as proposed by Koenker (1978), is an asymmetric loss function that imposes substantial penalties on observations that fall below the VaR threshold. The TLF's design ensures that the evaluation of VaR forecasts is sensitive to the magnitude of underestimations, making it a valuable tool for assessing the reliability of quantile forecasts in risk management applications.

$$\mathrm{TLF}_t^{\alpha} = \left(\alpha - I_{r_t < \mathrm{VaR}_t^{\alpha}}\right)\left(r_t - \mathrm{VaR}_t^{\alpha}\right) \tag{20}$$

To evaluate the joint prediction of VaR and ES, we use the Fissler-Ziegel Loss (FZL) function proposed by Fissler and Ziegel (2016). The FZL function is a novel loss function that measures the joint performance of VaR and ES forecasts. It rewards models that correctly predict the loss severity when the VaR threshold is exceeded. The FZL function is defined as:

$$\mathrm{FZL}_t^{\alpha} = \frac{1}{\alpha \mathrm{ES}_t^{\alpha}} I_{r_t < \mathrm{VaR}_t^{\alpha}}\left(r_t - \mathrm{VaR}_t^{\alpha}\right) + \frac{\mathrm{VaR}_t^{\alpha}}{\mathrm{ES}_t^{\alpha}} + \log\left(-\mathrm{ES}_t^{\alpha}\right) - 1 \tag{21}$$

Empirical analysis

Data and estimation. This study focuses on two prominent clean energy stock indices: the PowerShares WilderHill Clean Energy Portfolio (PBW) and the Invesco Global Clean Energy ETF (PBD). These indices were chosen for three primary reasons. First, both indices are designed to encapsulate the entire clean energy sector, covering a wide range of technologies and services within this industry. This comprehensive representation facilitates a more precise depiction of the sector's performance and trends. Second, as ETFs, PBW and PBD offer high liquidity, making them accessible to a diverse range of investors, including individual and institutional investors. This accessibility ensures a robust and active trading market for research purposes. Third, their long history in tracking the performance of the clean energy sector provides valuable insights into the risk characteristics and market dynamics of this sector.

Daily price data for PBW and PBD has been sourced from investing.com, spanning from the inception of each index until December 22, 2023. Specifically, PBW has approximately 4700 data points since March 7, 2005, while PBD has around 4100 data points since June 15, 2007. Data integrity checks confirmed that the raw daily price series are complete, with no missing values requiring imputation. The continuous compounded daily returns for both PBW and PBD are calculated by taking the natural logarithm of the difference between consecutive daily spot prices, multiplied by 100, denoted as $R_t = \left[lnP_t - lnP_{t-1}\right] * 100$.

The daily price changes and percentage returns for PBW and PBD are shown in Figs. 1 and 2, respectively. Visual inspection of these plots reveals no anomalous data points, such as those arising from data entry errors, that would warrant removal or adjustment. Consequently, the unfiltered return series are used for all subsequent analysis. A central focus of this study is the distinct risk profiles of long and short investment positions. It is important to clarify how the same return distribution is used to evaluate these opposing risks. The tail risk for a long position corresponds to the left tail of the return distribution, where large negative returns represent significant losses. Conversely, the risk for a short position, which profits from price declines, arises from large positive returns. Therefore, the tail risk for a short position

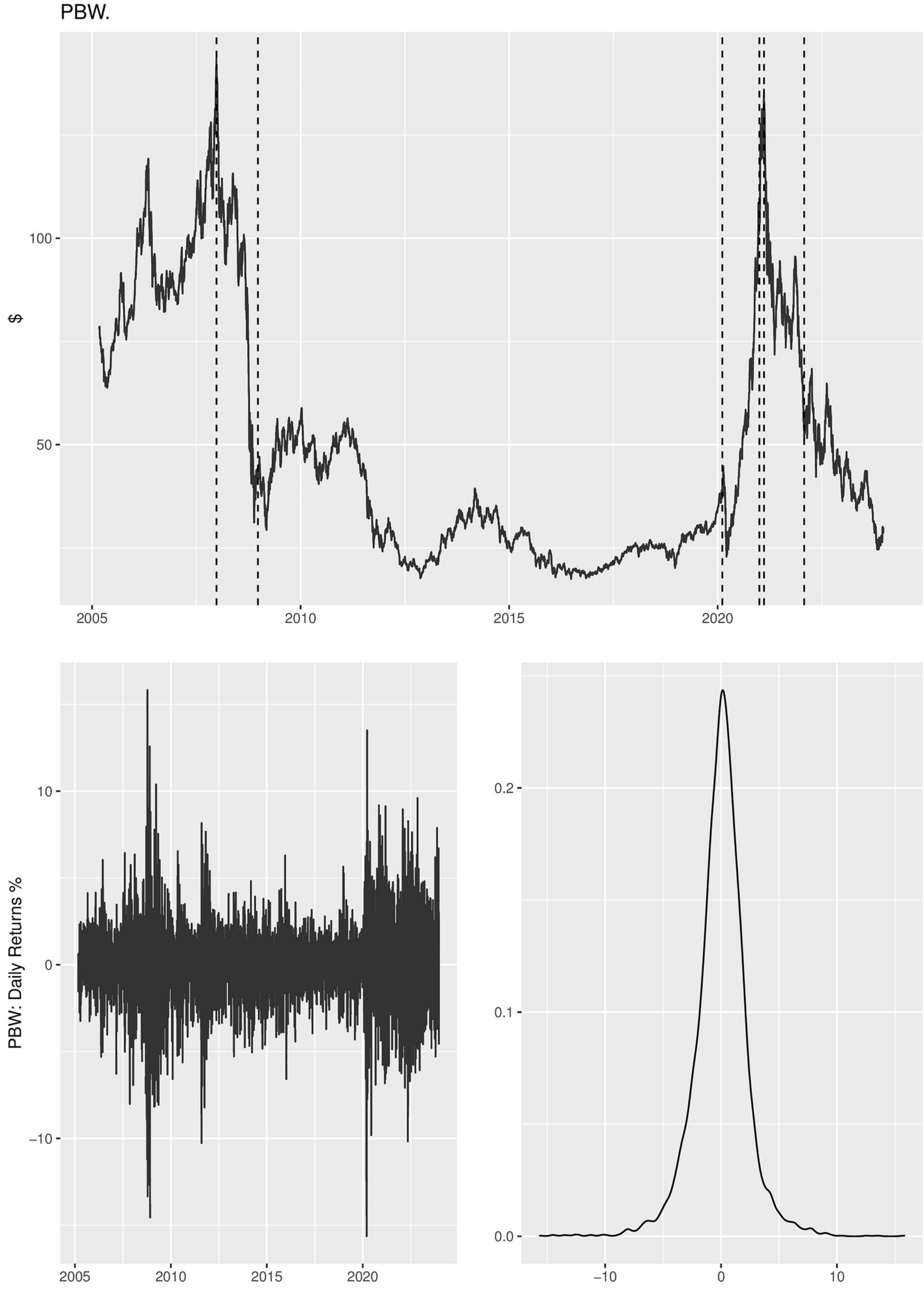

Fig. 1 PBW daily price and return. The graphs illustrate the daily price and return series for PBW, spanning from March 7, 2005 to December 22, 2023. Additionally, the return density graph is provided. The forecast windows of the three sub-samples are delineated by dashed lines.

corresponds to the right tail of the distribution. This study explicitly models both tails to investigate whether the statistical properties governing extreme negative returns are the same as those governing extreme positive returns, a distinction crucial for comprehensive risk management.

This distinction becomes particularly relevant when examining the historical volatility patterns of these indices. Both indices have exhibited substantial volatility, marked by significant peaks and troughs, indicative of broader market dynamics and the specific challenges faced by the clean energy sector. In particular, they

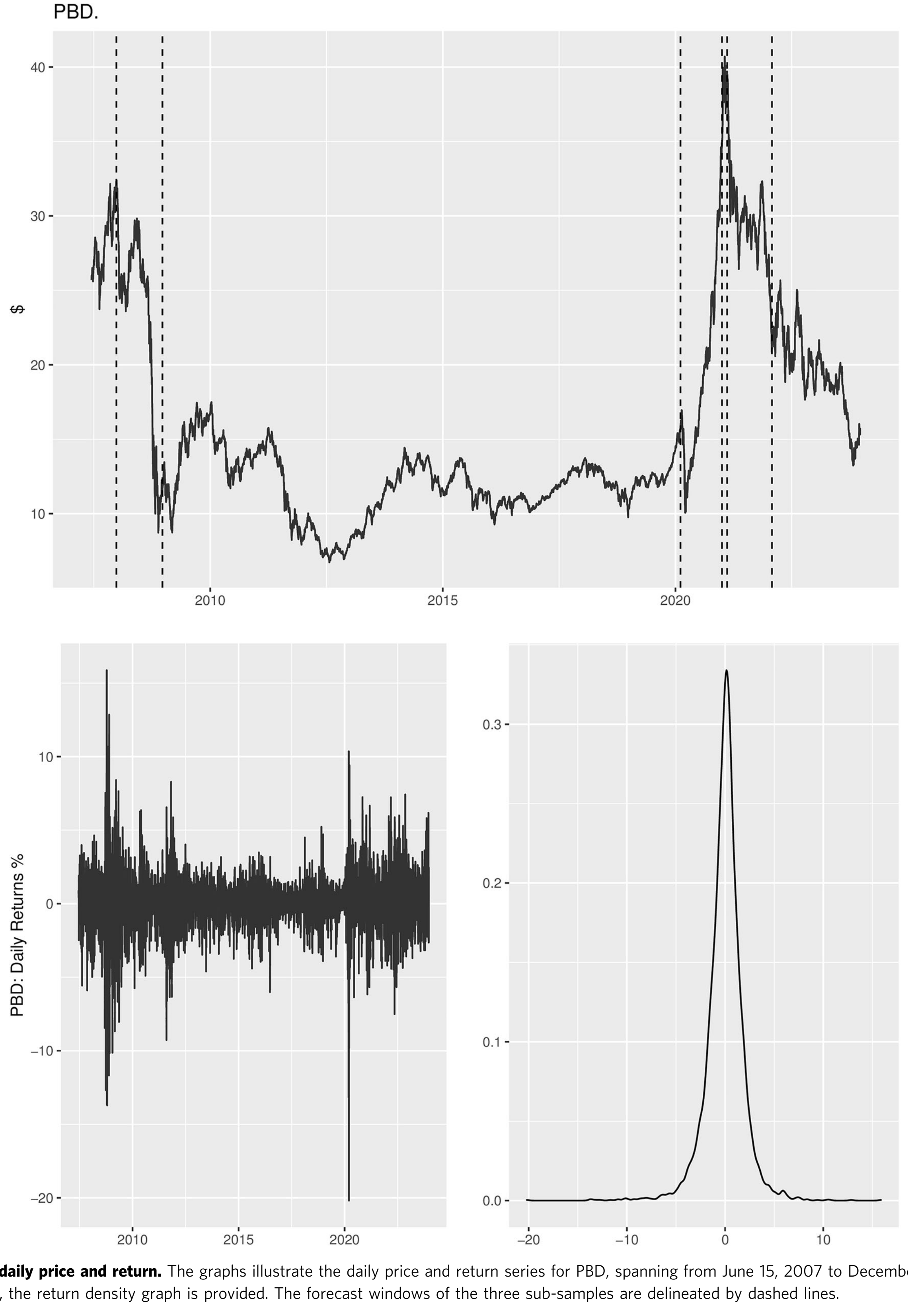

Fig. 2 PBD daily price and return. The graphs illustrate the daily price and return series for PBD, spanning from June 15, 2007 to December 22, 2023. Additionally, the return density graph is provided. The forecast windows of the three sub-samples are delineated by dashed lines.

experienced significant declines during the 2008 financial crisis and the initial phases of the COVID-19 pandemic. The more pronounced decline during the 2008 financial crisis was attributed to the systemic nature of the economic downturn and the sector's vulnerability to investor sentiment and credit availability. The COVID 19 pandemic caused an initial sharp decline, followed by a rapid recovery as the market anticipated a green economic resurgence. However, the subsequent decline may be influenced by evolving market priorities, supply chain disruptions, and the temporary competitiveness of traditional energy sources due to oil price volatility. The inherent volatility of the clean energy market, characterized by significant fluctuations, underlines the

Table 1 Data samples.

	No.of obs	Sample period	Forecast window
Panel A: PBW			
Full Sample	4762	Mar 07, 2005 - Dec 22, 2023	Mar 02, 2007 - Dec 22, 2023
Sample I	750	Dec 30, 2005 - Dec 22, 2008	Dec 27, 2007 - Dec 22, 2008
Sample II	750	Feb 13, 2018 - Dec 31, 2020	Feb 10, 2020 - Dec 31, 2020
Sample III	750	Mar 21, 2019 - Jan 28, 2022	Feb 10, 2021 - Jan 28, 2022
Panel B: PBD			
Full Sample	4189	Jun 15, 2007 - Dec 22, 2023	Jun 10, 2009 - Dec 22, 2023
Sample I	750	NA	NA
Sample II	750	Feb 13, 2018 - Dec 31, 2020	Feb 10, 2020 - Dec 31, 2020
Sample III	750	Mar 21, 2019 - Jan 28, 2022	Feb 10, 2021 - Jan 28, 2022

The table shows the number of data points, the start and end dates of each sample period, and the forecasting horizon for each segment. The Full sample contains all historical data. Samples I, II, and III are used to test the prediction of extreme risk in three turbulent periods: the 2008 financial crisis and the COVID-19 pandemic.

Table 2 Summary statistics.

	Full	Sample I	Sample II	Sample III
Panel A: PBW				
Mean	−0.020	−0.481	0.392	−0.381
Std	2.281	4.016	3.490	2.775
Min	−15.637	−14.555	−15.637	−6.830
Max	15.820	15.820	13.503	9.135
Skew	−0.305	−0.158	−0.936	0.017
Kurt	4.649	2.163	4.468	0.108
JB	4368.385	51.892	250.543	0.196
pval	(0.000)	(0.000)	(0.000)	(0.907)
LB(10)	25.391	5.587	22.820	13.483
pval	(0.005)	(0.849)	(0.011)	(0.198)
LM(10)	1158.554	82.104	63.172	41.452
pval	(0.000)	(0.000)	(0.000)	(0.000)
LM(20)	1194.308	95.954	68.352	45.025
pval	(0.000)	(0.000)	(0.000)	(0.001)
ADF	−15.940	−5.970	−6.768	−5.579
pval	(0.010)	(0.010)	(0.010)	(0.010)
Panel B: PBD				
Mean	−0.012	na	0.328	−0.229
Std	1.927	na	2.729	1.942
Min	−20.188	na	−20.188	-5.680
Max	15.876	na	10.355	6.665
Skew	−0.702	na	−2.200	0.033
Kurt	9.984	na	15.714	0.646
JB	17763.601	na	2825.761	4.800
pval	(0.000)	na	(0.000)	(0.091)
LB(10)	19.991	na	26.164	8.125
pval	(0.029)	na	(0.004)	(0.617)
LM(10)	1043.676	na	68.912	45.719
pval	(0.000)	na	(0.000)	(0.000)
LM(20)	1141.850	na	68.919	28.308
pval	(0.000)	na	(0.000)	(0.102)
ADF	−14.259	na	−6.564	−5.784
pval	(0.010)	na	(0.010)	(0.010)

The table presents the mean, standard deviation (std), minimum (min), maximum (max), and distributional shape measures (skewness and kurtosis) of daily percentage returns for PBW and PBD across the entire dataset and three distinct time intervals. The statistical tests employed include the Jarque-Bera test for normality, the ARCH (LM) test for up to 10th and 20th-order autoregressive conditional heteroskedasticity, and the augmented Dickey-Fuller (ADF) test for time series stationarity. The associated p-values are presented in parentheses. For the ADF test, all p values consistently fall below the 0.01 significance level.

need for robust risk management strategies by both market participants and regulators.

The PBW and PBD models are calibrated using a 500-observation estimation window to generate one-step-ahead VaR and ES forecasts for long and short positions on day 501. The choice of a 500-observation window for model estimation in the PBW and PBD indices is driven by two objectives: firstly, to ensure an adequate number of data points for accurate parameter estimation; secondly, to retain the period of the 2008 financial crisis for subsequent forecast evaluation. This approach is reinforced by a robustness check using a window of 1000 observations, which produces qualitatively similar results. Following this initial estimation, the window is moved forward by one day, and the model is re-estimated to predict day 502. This process is repeated until the dataset has been fully exhausted, resulting in 500 observations for model estimation and over 3500 for out-of-sample forecasting evaluation. The rolling window approach is utilized to incorporate the latest market information and eliminate outdated data, thereby enhancing the models' adaptability to current market conditions.

In order to evaluate the performance of the model under various market conditions, we divided the dataset into three sub-samples based on the observed market movements in Figs. 1 and 2. The start and end dates for each sample period can be found in Table 1. These sub-samples represent significant market events such as sharp declines during the 2008 financial crisis and COVID-19 pandemic, robust recoveries, and sustained declines after initial recoveries. Each sub-sample contains 500 observations for model estimation and 250 for out-of-sample forecasting, allowing a comprehensive analysis of the models' forecasting capabilities during periods of high volatility. The sub-sample periods are indicated by dashed lines in the price histories of PBW and PBD, as shown in the figures above. For PBD, we can't evaluate the out-of-sample forecast in Sample I because there are not enough data points to estimate the model.

Table 2 presents the summary statistics for the PBW and PBD return series across the full dataset and the three sub-sample periods. The mean daily returns for both indices are slightly negative during the Full sample period, reflecting a slight underperformance. However, the mean returns are notably negative in Sample I and Sample III, indicating periods of market downturns, while Sample II exhibits a positive mean return, indicating a period of market recovery. The largest standard deviation is observed in Sample I, which is consistent with the increased market volatility during the 2008 financial crisis. Interestingly, the lowest return is recorded in Sample II, which can be attributed to the market's reaction to the initial stages of the COVID-19 pandemic, where investor sentiment was particularly pessimistic despite the eventual market recovery. The rejection of the normality assumption by the Jarque-Bera test, due to the high kurtosis and negative skewness, underlines the need for models that take these non-normal characteristics into account. The ADF test confirms the stationarity of the return

Table 3 Volatility estimation.

GARCH-ST			GJRGARCH-ST			IGARCH-ST		
	Coef	*p*-val		Coef	*p*-val		Coef	*p*-val
Panel A: PBW								
μ	0.028	(0.268)	μ	0.004	(0.876)	μ	0.026	(0.297)
ar1	0.041	(0.002)	ar1	0.046	(0.000)	ar1	0.040	(0.004)
ω	0.036	(0.001)	ω	0.046	(0.001)	ω	0.025	(0.000)
α	0.076	(0.000)	α	0.049	(0.000)	α	0.080	(0.000)
β	0.918	(0.000)	β	0.914	(0.000)	β	0.920	NA
ξ	0.902	(0.000)	γ	0.055	(0.001)	ξ	0.901	(0.000)
ν	11.146	(0.000)	ξ	0.902	(0.000)	ν	10.452	(0.000)
			ν	11.035	(0.000)			
LB(10)	10.472	(0.400)	LB(10)	11.013	(0.356)	LB(10)	10.542	(0.394)
LM(10)	22.796	(0.012)	LM(10)	12.052	(0.282)	LM(10)	21.411	(0.018)
LM(20)	26.418	(0.152)	LM(20)	16.510	(0.685)	LM(20)	24.924	(0.204)
Panel B: PBD								
μ	0.042	(0.042)	μ	0.022	(0.321)	μ	0.042	(0.032)
ar1	0.018	(0.223)	ar1	0.023	(0.114)	ar1	0.018	(0.249)
ω	0.017	(0.004)	ω	0.022	(0.002)	ω	0.016	(0.001)
α	0.092	(0.000)	α	0.048	(0.000)	α	0.093	(0.000)
β	0.907	(0.000)	β	0.907	(0.000)	β	0.907	NA
ξ	0.894	(0.000)	γ	0.081	(0.000)	ξ	0.894	(0.000)
ν	7.307	(0.000)	ξ	0.893	(0.000)	ν	7.231	(0.000)
			ν	7.374	(0.000)			
LB(10)	10.952	(0.361)	LB(10)	10.886	(0.366)	LB(10)	10.963	(0.360)
LM(10)	10.674	(0.383)	LM(10)	8.533	(0.577)	LM(10)	10.360	(0.409)
LM(20)	14.218	(0.819)	LM(20)	10.656	(0.955)	LM(20)	14.035	(0.829)

The table provides the estimated parameters and corresponding *p*-values, enclosed in brackets, for the GARCH, GJRGARCH, and IGARCH models, which incorporate skewed *t*-distributed innovations, for the PBW and PBD returns throughout the entire sample period. The diagnostics for the standardized residuals encompass the Ljung-Box (LB) test to assess autocorrelation up to the 10th lag, as well as the ARCH (LM) test to examine autoregressive conditional heteroskedasticity for orders 10 and 20.

series, while the ARCH portmanteau test reveals significant volatility clustering, emphasizing the importance of capturing these features for accurate tail risk forecasting.

Table 3 presents the estimation results for the GARCH, GJRGARCH, and IGARCH models, each specified with an AR(1) mean equation and a skewed *t*-distribution for the innovations. For both the PBW and PBD indices, the significant AR(1) coefficient suggests the presence of autocorrelation in the return series.

The results reveal several key features of clean energy volatility dynamics. First, for both the GARCH and GJRGARCH models, the sum of the ARCH and GARCH coefficients $\alpha + \beta$ is close to one, signifying a high degree of volatility persistence. Second, the leverage parameter γ in the GJRGARCH model is positive and significant for both indices. This confirms a pronounced leverage effect, wherein negative shocks have a more substantial impact on future volatility than positive shocks of the same magnitude. To account for the high persistence observed in the data, the IGARCH model was selected. While a Fractionally Integrated GARCH (FIGARCH) model Baillie et al. (1996) was initially considered for its ability to capture long-memory effects, preliminary analysis showed a long-memory parameter close to 0.99. Given that this indicates a very slow decay of shocks, the more parsimonious IGARCH model was chosen as a robust specification to account for this near-unit-root behavior in the volatility process. This is particularly relevant for clean energy stocks, whose volatility is influenced by both immediate market news and long-term trends in technology and regulation.

The estimated parameters for the skewed *t*-distribution confirm the presence of significant fat tails and negative skewness in the return distributions for both indices. Importantly, diagnostic tests on the standardized residuals from all estimated models show no remaining significant autocorrelation or ARCH effects at a lag of 20, indicating that the chosen model specifications are well-defined and have successfully captured the conditional dynamics of the data.

Results. We first assess the accuracy of volatility forecasts for the PBW and PBD indices based on the GARCH, IGARCH, and GJRGARCH models, which include the innovations based on the normal and skewed *t*-distributions. The parameters are estimated by quasi-maximum likelihood estimation (QMLE). This method is standard practice in financial econometrics as it provides consistent and asymptotically normal estimators even if the specified distribution of the innovations is incorrect, provided the mean and variance equations are correctly specified (Bollerslev and Wooldridge, 1992; Hamilton, 2020). The squared daily returns are used as a reference to evaluate the forecast accuracy. According to Table 4, the QLIKE loss function, with lower values indicating higher precision, reveals that the GJRGARCH, particularly with skewed *t*-innovation, provides the most accurate volatility forecasts for both indices. This model's enhanced performance is attributed to its ability to differentiate between the effects of positive and negative returns on volatility, aligning with market behavior during various market trends. Overall, the models with skewed *t* innovation perform better than those with normal innovation, suggesting that non-normal innovation should be taken into account for more accurate volatility forecasting in clean energy stock markets.

The performance of the VaR and ES forecasts for PBW and PBD is assessed at the 97.5% and 99% confidence levels, employing a robust set of evaluation criteria. These include AE ratios, *p*-values for various backtesting tests, and the MaxAD metric (McAleer and Medeiros, 2008), which measures the maximum absolute deviation from VaR forecasts. The MCS test at a 90% confidence level evaluates the mean values of the Tick and FZL functions, providing a stringent assessment of model accuracy. The VaR and ES forecasts' mean and standard deviations, along with backtesting outcomes, are detailed in Tables 5 and 6 for long positions in PBW and PBD over the entire out-of-sample forecast periods. A more granular analysis of sub-sample periods at the 97.5% confidence level is given in Tables 7 and 8 for PBW and PBD, respectively. Due to the small sample sizes in these sub-samples, which can affect the power of p-value tests, we consider the AE ratio, ADMax, and loss function values as the main indicators of model performance. The key insights for long positions are as follows.

First, the efficacy of various innovation distributions within the GARCH model framework is critical to accurate forecasting. Models based on the normal distribution consistently underperform, as evidenced by elevated AE ratios and frequent rejection of VaR and ES p-value tests, indicating potential model misspecification. In the context of high confidence level VaR predictions, the historical simulation approach is outperformed by both the Cornish-Fisher expansions and the skewed t. The skewed t distribution, when evaluated using the loss functions, is found to offer the most accurate combined forecasts for VaR and ES. Conversely, the Cornish-Fisher expansion, while characterized by the highest mean and standard deviation for VaR and ES forecasts, consistently delivers the most conservative estimates of tail risk. This is attributed to the lowest AE ratio and the smallest Mean Absolute Deviation (MAD) observed in the model's performance. The conservative nature of the Cornish-Fisher expansion suggests its suitability for risk-averse investors or institutions that prioritize the minimization of potential losses during periods of market stress.

Second, the IGARCH model, which incorporates long-term memory into volatility, produces higher VaR and ES forecasts over the entire sample period for both PBW and PBD. During the 2008 Global Financial Crisis (GFC) period, the IGARCH model outperforms the GJRGARCH model in terms of AE ratio, tick loss, and FZL metrics. This suggests that it provides a more accurate representation of tail risk during this period of extreme market stress. This can be attributed to the IGARCH model's ability to adapt to the slow decay of shocks, which is particularly pertinent during prolonged periods of market instability. However, despite its performance during the GFC, the GJRGARCH model generally produces more accurate VaR and ES forecasts. The integration of the GJRGARCH model with skewed t innovation outperforms all other models based on the evaluation of tick and FZL function. This improved performance is further corroborated by the results of the QLIKE test, which indicates that it generates the most accurate volatility forecasts.

Third, a comparative analysis of the sub-sample periods, with key descriptive statistics presented in Table 2 and detailed backtesting results in Table 7, reveals distinct risk characteristics across different market regimes. The GFC (Sample I) exhibits the highest overall market volatility, with the largest standard deviations in daily returns and VaR/ES forecasts, alongside significantly higher AE ratios indicating frequent VaR breaches

Table 4 Volatility forecasts evaluation.

	Full	Sample I	Sample II	Sample III
Panel A: PBW				
GARCH-N	2.373	3.320	3.450	**2.976**
GARCH-ST	2.372	3.320	3.428	**2.975**
gjrGARCH-N	2.373	3.297	3.535	**2.976**
gjrGARCH-ST	**2.368**	**3.288**	3.515	**2.980**
iGARCH-N	2.374	3.301	3.409	2.981
iGARCH-ST	2.371	3.303	**3.396**	**2.978**
Panel B: PBD				
GARCH-N	1.692	na	2.697	2.209
GARCH-ST	1.687	na	2.662	2.203
gjrGARCH-N	1.684	na	2.802	2.200
gjrGARCH-ST	**1.680**	na	2.770	**2.190**
iGARCH-N	1.697	na	2.661	2.210
iGARCH-ST	1.690	na	**2.651**	2.202

The table presents the mean values of the QLIKE loss function across different sample forecast durations. The forecasted volatility of each model is evaluated against the daily squared returns, acting as a benchmark for realized volatility. The MCS test is applied to assess the precision of the forecasts at a 90% confidence level. Models highlighted in bold denote those included in the superior set due to their statistically equivalent volatility forecasts.

Table 5 Full sample VaR and ES results for long PBW positions.

	GARCH				GJRGARCH				IGARCH			
	N	ST	HS	CF	N	ST	HS	CF	N	ST	HS	CF
Panel A: Confidence level 97.5%												
mVaR	−4.102	-4.376	−4.377	−4.443	−4.086	−4.387	−4.304−	4.404	−4.219	−4.512	−4.452	−4.596
stdVaR	2.038	2.167	2.177	2.253	2.071	2.230	2.182	2.276	2.148	2.263	2.254	2.376
mES	−4.897	−5.599	−5.518	-5.581	−4.871	−5.598	−5.396	−5.518	−5.036	−5.826	−5.666	−5.798
stdES	2.432	2.837	2.847	2.925	2.468	2.914	2.840	2.956	2.564	2.970	2.981	3.082
AE	1.389	1.117	1.107	1.098	1.370	1.126	1.192	1.164	1.389	1.089	1.107	1.051
LR_{uc}	0.000	0.230	0.269	0.313	0.000	0.196	0.051	0.095	0.000	0.361	0.269	0.596
LR_{cc}	0.001	0.479	0.537	0.596	0.000	0.423	0.088	0.158	0.001	0.509	0.537	0.726
DQ	0.000	0.300	0.136	0.178	0.000	0.610	0.052	0.270	0.000	0.016	0.010	0.037
ER	0.000	0.622	0.434	0.315	0.000	0.892	0.527	0.650	0.000	0.898	0.593	0.492
ESR	0.000	0.527	0.376	0.486	0.001	0.706	0.309	0.496	0.003	0.926	0.663	0.862
ADMax	6.918	6.335	6.980	6.451	6.682	5.982	6.677	6.213	6.466	5.857	6.631	5.900
Tick	0.141	0.139	0.140	0.139	0.139	**0.137**	0.137	0.137	0.141	0.140	0.141	0.140
FZL	1.700	1.669	1.669	1.666	1.688	**1.648**	1.659	1.657	1.706	1.671	1.680	1.677
Panel B: Confidence level 99%												
mVaR	−4.873	−5.478	−5.364	v5.561	−4.847	−5.479	−5.240	−5.499	−5.011−	5.686	−5.467	−5.773
stdVaR	2.420	2.755	2.707	2.897	2.456	2.830	2.743	2.926	2.552	2.882	2.829	3.053
mES	−5.586	−6.730	−6.381	−6.669	−5.551	−6.717	−6.211	−6.582	−5.743	−7.051	−6.548	−6.950
stdES	2.774	3.492	3.402	3.594	2.813	3.581	3.375	3.637	2.925	3.661	3.564	3.784
AE	1.924	1.126	1.290	1.103	1.924	1.126	1.361	1.103	1.947	1.056	1.220	1.079
LR_{uc}	0.000	0.417	0.068	0.507	0.000	0.417	0.025	0.507	0.000	0.717	0.163	0.607
LR_{cc}	0.000	0.416	0.084	0.475	0.000	0.613	0.078	0.475	0.000	0.579	0.199	0.530
DQ	0.000	0.243	0.052	0.245	0.000	0.786	0.311	0.764	0.000	0.035	0.066	0.227
ER	0.000	0.093	0.073	0.052	0.000	0.606	0.010	0.002	0.000	0.631	0.034	0.213
ESR	0.088	0.620	0.354	0.573	0.015	0.777	0.278	0.598	0.114	0.894	0.495	0.748
ADMax	5.925	4.801	4.636	4.934	5.899	4.802	4.988	5.087	5.389	4.161	4.387	4.217
Tick	0.069	0.066	0.066	0.067	0.067	**0.065**	0.066	0.066	0.069	0.067	0.066	0.068
FZL	1.931	1.847	1.850	1.847	1.913	**1.818**	1.848	1.839	1.936	1.846	1.853	1.856

The table presents the mean values and standard deviations of VaR and ES forecasts at 97.5% (Panel A) and 99% (Panel B) confidence levels for long positions in PBW. Additionally, it includes backtesting outcomes for three GARCH variants paired with different distributions: normal (N), skewed t (ST), historical simulation (HS), or Cornish-Fisher expansion (CF), throughout the entire forecasting horizon. The table details the AE ratio, the p-values for the LR_{uc}, LR_{cc}, DQ, one-sided ER, one-sided Intercept ESR tests, alongside the absolute maximum deviation (ADMax) and mean values of the tick and FZL metrics. Models highlighted in bold denote those included in the superior set of models, which have statistically comparable VaR forecasts based on either the tick loss function or joint VaR and ES forecasts based on the FZL function at a 90% confidence level.

Table 6 Full sample VaR and ES Results for Long PBD Positions.

	GARCH				GJRGARCH				IGARCH			
	N	ST	HS	CF	N	ST	HS	CF	N	ST	HS	CF
Panel A: Confidence level 97.5%												
mVaR	−2.929	−3.161	−3.320	−3.286	−2.925−	3.159	−3.260	-3.261	−3.018	−3.246	−3.368	−3.411
stdVaR	1.400	1.553	1.732	1.628	1.481	1.667	1.804	1.703	1.498	1.611	1.817	1.744
mES	−3.502	−4.186	−4.234	−4.271	−3.490	−4.142	−4.146	−4.211	−3.607	−4.352	−4.344	−4.460
stdES	1.669	2.149	2.151	2.237	1.763	2.287	2.223	2.331	1.785	2.229	2.269	2.396
AE	1.366	1.182	1.041	1.030	1.323	1.139	1.095	1.073	1.279	1.106	1.008	0.976
LR_{uc}	0.001	0.085	0.692	0.771	0.003	0.187	0.362	0.480	0.009	0.311	0.935	0.814
LR_{cc}	0.001	0.172	0.504	0.539	0.002	0.165	0.302	0.384	0.030	0.595	0.969	0.963
DQ	0.001	0.049	0.405	0.390	0.009	0.134	0.625	0.542	0.017	0.230	0.741	0.825
ER	0.000	0.878	0.450	0.544	0.000	0.930	0.788	0.873	0.000	0.926	0.444	0.816
ESR	0.000	0.494	0.507	0.560	0.000	0.601	0.525	0.606	0.003	0.758	0.651	0.828
ADMax	7.518	5.751	4.455	5.085	6.916	4.755	4.023	4.598	6.941	5.712	4.095	4.283
Tick	0.108	0.106	0.107	0.106	0.105	**0.103**	0.104	0.104	0.108	0.106	0.107	0.107
FZL	1.446	1.387	1.395	1.390	1.417	**1.365**	1.370	1.369	1.452	1.395	1.409	1.404
Panel B: Confidence level 99%												
mVaR	−3.485	−4.053	−4.128	−4.232	−3.473	−4.020	-4.080	−4.177	−3.589	-4.196	−4.197	−4.416
stdVaR	1.661	2.050	2.037	2.194	1.755	2.188	2.155	2.287	1.777	2.126	2.176	2.351
mES	−3.999	−5.161	-4.877	−5.224	-3.980	−5.071	−4.774	−5.130	−4.118	−5.412	−5.029	−5.477
stdES	1.902	2.754	2.472	2.863	2.009	2.914	2.590	2.980	2.035	2.857	2.615	3.067
AE	2.223	1.355	1.166	1.166	2.196	1.274	1.111	1.003	2.060	1.193	1.193	0.976
LR_{uc}	0.000	0.040	0.325	0.325	0.000	0.109	0.504	0.985	0.000	0.254	0.254	0.882
LR_{cc}	0.000	0.112	0.505	0.371	0.000	0.246	0.624	0.688	0.000	0.306	0.438	0.657
DQ	0.000	0.000	0.000	0.000	0.000	0.109	0.136	0.598	0.000	0.024	0.006	0.068
ER	0.000	0.012	0.486	0.569	0.000	0.153	0.829	0.996	0.000	0.007	0.754	0.974
ESR	0.000	0.740	0.300	0.736	0.000	0.821	0.359	0.820	0.010	0.869	0.428	0.882
ADMax	0.906	0.707	0.812	0.727	0.803	0.618	0.741	0.723	0.905	0.697	0.783	0.759
Tick	0.055	0.050	0.051	0.051	0.052	**0.048**	0.049	0.049	0.055	0.050	0.051	0.052
FZL	1.752	1.566	1.579	1.577	1.705	**1.541**	1.557	1.551	1.761	1.569	1.608	1.603

The table presents the mean values and standard deviations of VaR and ES forecasts at 97.5% (Panel A) and 99% (Panel B) confidence levels for long positions in PBD. Additionally, it includes backtesting outcomes for three GARCH variants paired with different distributions: normal (N), skewed *t* (ST), historical simulation (HS), or Cornish-Fisher expansion (CF), throughout the entire forecasting horizon. The table details the AE ratio, the *p*-values for the LR_{uc}, LR_{cc}, DQ, one-sided ER, one-sided Intercept ESR tests, alongside the absolute maximum deviation (ADMax) and mean values of the tick and FZL metrics. Models highlighted in bold denote those included in the superior set of models, which have statistically comparable VaR forecasts based on either the tick loss function or joint VaR and ES forecasts based on the FZL function at a 90% confidence level.

Table 7 Sub-sample VaR and ES Results for Long PBW Positions at 97.5% Confidence.

	GARCH				GJRGARCH				IGARCH			
	N	ST	HS	CF	N	ST	HS	CF	N	ST	HS	CF
Panel A: Sample I												
mVaR	−6.470−	6.904	−6.974	−7.137	−6.479	−7.027	−7.040	−7.175	−6.857	−7.234	−7.200	−7.627
stdVaR	4.052	4.355	4.329	4.460	4.057	4.475	4.371	4.491	4.060	4.329	4.344	4.454
mES	−7.725	−8.731	−8.832	−9.049	−7.730	−8.863	−8.800	−9.118	−8.184	−9.210	−9.245	−9.753
stdES	4.834	5.524	5.423	5.602	4.835	5.644	5.373	5.667	4.845	5.479	5.457	5.572
AE	2.709	2.072	1.912	1.753	2.231	1.753	1.753	1.753	2.072	1.434	1.434	0.956
ADMax	1.083	0.987	1.003	0.972	1.243	1.025	1.047	0.931	0.932	0.960	1.057	1.076
Tick	0.223	0.212	0.210	0.209	0.219	0.209	0.210	0.208	0.208	0.203	0.206	0.204
FZL	2.275	2.175	2.155	2.141	2.238	2.138	2.142	2.126	2.143	2.099	2.114	2.095
Panel B: Sample II												
mVaR	−5.902	−6.613	−6.579	−6.893	−5.730	-6.354	-6.226	−6.649	−6.120−	6.813	−6.772	−7.155
stdVaR	2.884	3.128	3.214	3.234	3.197	3.601	3.430	3.519	2.917	3.202	3.248	3.265
mES	−7.070	−9.088	−9.090	−9.264	−6.860	−8.762	-8.641	−8.988	−7.329−	9.409	−9.333	−9.608
stdES	3.427	4.048	4.191	4.169	3.795	4.691	4.492	4.552	3.467	4.130	4.235	4.198
AE	1.120	1.120	1.120	1.120	1.280	1.120	1.280	1.120	1.120	1.120	1.120	1.120
ADMax	6.918	6.335	6.980	6.451	6.682	5.982	6.677	6.213	6.466	5.857	6.631	5.900
Tick	0.269	0.267	0.280	0.271	0.257	0.250	0.264	0.258	0.267	0.264	0.278	0.269
FZL	2.459	2.368	2.431	2.393	2.457	2.339	2.421	2.384	2.418	2.335	2.404	2.363
Panel C: Sample III												
mVaR	−5.304	−5.575	−5.360	-6.074	−5.512	−5.907	−5.446	-6.250	−5.380	−5.657−	5.365	−6.180
stdVaR	1.476	1.602	1.528	1.780	1.549	1.754	1.617	1.841	1.498	1.625	1.571	1.794
mES	−6.376	−7.669	−7.873	−8.211−	6.619	−8.136	−7.956	-8.454	−6.465	−7.846	−7.958	−8.377
stdES	1.757	2.251	2.366	2.474	1.843	2.447	2.441	2.545	1.783	2.272	2.384	2.476
AE	1.606	1.124	1.446	0.964	0.964	0.803	1.285	0.482	1.446	1.124	1.446	0.803
ADMax	1.928	1.819	1.981	1.467	1.706	1.510	1.925	1.237	1.952	1.819	2.078	1.481
Tick	0.155	0.155	0.156	0.156	0.152	0.154	0.154	0.158	0.155	0.155	0.159	0.157
FZL	1.903	1.897	1.915	1.900	1.868	1.883	1.900	1.906	1.897	1.901	1.932	1.905

The table presents the mean values and standard deviations of VaR and ES forecasts at 97.5% confidence level for long positions in PBW. Additionally, it includes backtesting outcomes for three GARCH variants paired with different distributions: normal (N), skewed *t* (ST), historical simulation (HS), or Cornish-Fisher expansion (CF) over the sub-sample forecast horizons. The table shows the AE ratio, the absolute maximum deviation (ADMax) and mean values of the tick and FZL metrics.

and sustained systemic risk. In contrast, the COVID-19 period (Sample II) presents a different risk profile characterized by sharp, V-shaped market reactions rather than sustained volatility. While overall volatility was lower than the GFC, this period featured the most extreme single-day negative return and larger maximum deviations from VaR forecasts (ADMax), indicating a crisis defined by singular, extreme shocks rather than persistent high volatility. Sample III shows market adaptation to a new risk environment where mean VaR and ES forecasts remain high but with significantly lower standard deviations, suggesting more stable day-to-day risk fluctuations due to market resilience. These differences highlight the importance of using risk models robust to different crisis types-whether prolonged, systemic downturns or sharp, sudden shocks.

Next, we assess the prediction accuracy for short positions in PBW and PBD, as shown in Tables 9 and 10. The difference in prediction accuracy between forecasting short position for PBW and PBD are less pronounced than those for long positions. The IGARCH model produces more conservative VaR and ES forecasts than the GARCH and GJRGARCH models for both indices. At the 99% confidence level, the IGARCH model combined with a skewed *t* distribution yields the most accurate forecasts, as assessed by the tick and FZL functions. On the other hand, the GJRGARCH model, which surpasses the GARCH and

Table 8 Sub-sample VaR and ES Results for Long PBD Positions at 97.5% Confidence.

	GARCH				GJRGARCH				IGARCH			
	N	ST	HS	CF	N	ST	HS	CF	N	ST	HS	CF
Panel A: Sample II												
mVaR	−4.124	−4.685	−5.188	−5.118	−4.056	−4.532	−5.048	−5.005	−4.283	−4.720	−5.293	−5.344
stdVaR	2.928	3.372	3.712	3.469	3.332	3.944	4.250	3.891	3.053	3.384	3.836	3.632
mES	−4.950	−6.773	−6.823	−7.259	−4.863	−6.535	−6.604	−7.121	−5.140	−6.838	−7.010	−7.621
stdES	3.492	4.636	4.559	4.673	3.973	5.403	5.062	5.236	3.640	4.654	4.696	4.917
AE	1.280	1.280	1.280	1.280	1.280	1.280	1.280	1.280	1.280	1.280	1.280	1.280
ADMax	7.518	5.751	4.455	5.085	6.916	4.755	4.023	4.598	6.941	5.712	4.095	4.283
Tick	0.226	0.215	0.220	0.220	0.219	0.205	0.207	0.214	0.219	0.213	0.215	0.211
FZL	2.254	2.032	2.084	2.083	2.326	2.080	2.113	2.134	2.174	2.017	2.049	2.018
Panel B: Sample III												
mVaR	−3.580	−3.683	−4.214	−4.326	−3.696	−3.864	−4.227	−4.427	−3.674	−3.754−	4.219	−4.464
stdVaR	1.225	1.270	1.427	1.565	1.293	1.371	1.489	1.626	1.254	1.303	1.435	1.600
mES	−4.308	−5.327	−5.850	−6.180	−4.444	−5.579	−5.944	−6.337	−4.419	−5.487	−5.918	−6.404
stdES	1.455	1.836	2.098	2.349	1.533	1.961	2.165	2.423	1.489	1.891	2.119	2.405
AE	2.080	1.760	1.120	0.960	1.280	1.280	1.120	0.960	1.760	1.440	1.120	0.960
ADMax	1.812	1.825	1.494	1.425	1.567	1.532	1.291	1.163	1.856	1.826	1.540	1.458
Tick	0.116	0.115	0.116	0.115	0.113	0.113	0.116	0.114	0.115	0.115	0.117	0.117
FZL	1.638	1.607	1.596	1.581	1.575	1.566	1.584	1.569	1.631	1.612	1.612	1.601

The table presents the mean values and standard deviations of VaR and ES forecasts at 97.5% confidence level for long positions in PBD. Additionally, it includes backtesting outcomes for three GARCH variants paired with different distributions: normal (N), skewed *t* (ST), historical simulation (HS), or Cornish-Fisher expansion (CF) over the sub-sample forecast horizons. The table shows the AE ratio, the absolute maximum deviation (ADMax) and mean values of the tick and FZL metrics.

Table 9 Full sample VaR and ES Results for Short PBW Positions.

	GARCH				GJRGARCH				IGARCH			
	N	ST	HS	CF	N	ST	HS	CF	N	ST	HS	CF
Panel A: Confidence level 97.5%												
mVaR	−4.146	−3.963	−3.934	−3.945	−4.056	−3.877	−3.872	−3.880	−4.253	−4.054	−3.962	−4.031
stdVaR	2.075	2.025	2.007	1.982	2.082	2.055	2.044	2.008	2.190	2.123	2.109	2.092
mES	−4.941	−4.927	−4.814	−4.764−	4.841	−4.811	−4.758	−4.703	−5.069	−5.078	−4.803	−4.881
stdES	2.470	2.559	2.423	2.442	2.480	2.613	2.494	2.498	2.606	2.687	2.518	2.579
AE	0.985	1.136	1.201	1.154	0.985	1.183	1.229	1.173	0.901	1.089	1.258	1.107
LR_{uc}	0.879	0.165	0.041	0.115	0.879	0.064	0.020	0.078	0.293	0.361	0.010	0.269
LR_{cc}	0.956	0.274	0.105	0.281	0.172	0.095	0.026	0.109	0.494	0.405	0.024	0.501
DQ	0.825	0.238	0.144	0.232	0.235	0.170	0.043	0.149	0.822	0.553	0.094	0.761
ER	0.005	0.294	0.062	0.004	0.000	0.010	0.032	0.000	0.024	0.702	0.122	0.068
ESR	0.162	0.196	0.042	0.022	0.051	0.075	0.024	0.013	0.431	0.499	0.073	0.210
ADMax	4.739	5.212	5.376	5.545	4.992	5.387	5.392	5.263	4.210	4.815	4.922	5.064
Tick	**0.129**	**0.129**	0.130	0.129	**0.129**	**0.129**	0.130	**0.129**	**0.129**	**0.128**	0.130	**0.129**
FZL	**1.555**	**1.553**	1.569	1.561	1.568	1.571	1.581	1.575	**1.554**	**1.548**	1.566	**1.554**
Panel B: Confidence level 99%												
mVaR	−4.917	-4.838	−4.735	−4.763	−4.817	−-4.734	−4.665	−4.700	−5.045	−4.975	−4.752−	4.877
stdVaR	2.458	2.500	2.428	2.431	2.468	2.541	2.485	2.482	2.594	2.624	2.524	2.567
mES	−5.630	−5.814	−5.455	−5.546	−5.521	−5.677−	5.421−	5.488	−5.777	−6.028	−5.447	−5.695
stdES	2.812	3.067	2.730	2.897	2.825	3.138	2.852	2.985	2.967	3.225	2.840	3.060
AE	1.126	1.173	1.337	1.314	1.361	1.572	1.619	1.455	1.079	1.079	1.220	1.197
LR_{uc}	0.417	0.269	0.035	0.049	0.025	0.001	0.000	0.005	0.607	0.607	0.163	0.211
LR_{cc}	0.613	0.480	0.105	0.139	0.012	0.000	0.000	0.001	0.716	0.716	0.344	0.411
DQ	0.741	0.641	0.259	0.320	0.004	0.000	0.000	0.000	0.804	0.804	0.513	0.580
ER	0.000	0.097	0.001	0.000	0.001	0.258	0.002	0.000	0.004	0.258	0.000	0.009
ESR	0.030	0.176	0.022	0.027	0.016	0.070	0.006	0.027	0.147	0.467	0.007	0.077
ADMax	3.429	3.339	3.690	3.482	3.969	4.444	4.457	4.365	3.537	3.391	3.495	3.468
Tick	**0.061**	**0.061**	**0.062**	0.062	**0.062**	**0.062**	0.063	0.062	**0.061**	**0.061**	**0.061**	**0.061**
FZL	**1.744**	**1.739**	1.753	1.754	1.770	1.779	1.798	1.787	**1.737**	**1.734**	**1.742**	**1.742**

The table presents the mean values and standard deviations of VaR and ES forecasts at 97.5% (Panel A) and 99% (Panel B) confidence levels for short positions in PBW. Additionally, it includes backtesting outcomes for three GARCH variants paired with different distributions: normal (N), skewed *t* (ST), historical simulation (HS), or Cornish-Fisher expansion (CF), throughout the entire forecasting horizon. The table details the AE ratio, the *p*-values for the LR_{uc}, LR_{cc}, DQ, one-sided ER, one-sided Intercept ESR tests, alongside the absolute maximum deviation (ADMax) and mean values of the tick and FZL metrics. Models highlighted in bold denote those included in the superior set of models, which have statistically comparable VaR forecasts based on either the tick loss function or joint VaR and ES forecasts based on the FZL function at a 90% confidence level.

IGARCH models in forecasting long positions, does not show equivalent accuracy for VaR and ES at the 99% confidence level. This discrepancy may be due to the asymmetric response of the GJRGARCH model to market shocks, which is less relevant for short positions.

Then, we delve into the comparative analysis of VaR and ES forecasts to enhance our understanding of risk assessment for the PBW and PBD indices. We adhere to the methodology proposed by Patra (2021) by calculating the ES to VaR ratio at a 99% confidence level, which serves as a critical metric for evaluating the effectiveness of risk models. The results, presented in Table 11, reveal a nuanced picture of risk sensitivity across different market conditions. The ratio, which stands at approximately 1.15 for a normal distribution of innovations, escalates dramatically for non-normal distributions, varying among models and time-periods. Notably, the third sample period exhibits the highest ratios, suggesting that market conditions during this period were particularly conducive to a more pronounced risk profile. The study further uncovers that the ES consistently outperforms the VaR when estimated by the GJRGARCH model with skewed *t*-innovation, surpassing it by over 40% for both long and short positions. This large gap indicates that the ES measure has higher sensitivity to market volatility, which can provide a more reliable risk assessment in uncertain periods. Additionally, as shown in Table 12, the transition from VaR to ES, which is a shift from a 99.5% to a 97.5% confidence level, leads to a modest yet notable increase in risk prediction, particularly under normal innovation scenarios. The increase ranges from 2 to 3% for long positions in PBW and PBD indices estimated by GJRGARCH model, and a similar increase for short positions estimated by IGARCH model. These results demonstrate that skewed *t* distribution can be used to capture potential losses beyond VaR threshold.

The VaR forecast plots presented in Figs. 3 and 4 provide valuable insights into the dynamic risk profiles of clean energy ETFs and the comparative performance of different GARCH specifications. Several important patterns emerge from the visual

Table 10 Full sample VaR and ES Results for Short PBD Positions.

	GARCH				GJRGARCH				IGARCH			
	N	**ST**	**HS**	**CF**	**N**	**ST**	**HS**	**CF**	**N**	**ST**	**HS**	**CF**
Panel A: Confidence level 97.5%												
mVaR	−3.015	−2.888	−2.898	−2.828	−2.940	−2.816−	2.851	−2.761	−3.099	−2.940	−2.917	−2.892
stdVaR	1.411	1.377	1.369	1.328	1.480	1.456	1.452	1.415	1.510	1.437	1.461	1.418
mES	−3.588	−3.701	−3.506	−3.492	−3.505	−3.584	−3.455	−3.408	−3.688	−3.810	−3.497	−3.588
stdES	1.680	1.847	1.716	1.721	1.763	1.953	1.842	1.846	1.798	1.931	1.800	1.841
AE	0.867	1.139	1.128	1.171	0.943	1.160	1.214	1.225	0.857	1.063	1.117	1.128
LR_{uc}	0.187	0.187	0.223	0.105	0.578	0.128	0.044	0.034	0.153	0.547	0.265	0.223
LR_{cc}	0.411	0.419	0.476	0.268	0.398	0.187	0.055	0.077	0.350	0.809	0.436	0.476
DQ	0.575	0.322	0.253	0.182	0.409	0.343	0.078	0.065	0.386	0.596	0.118	0.366
ER	0.003	0.336	0.265	0.558	0.000	0.527	0.177	0.172	0.018	0.147	0.011	0.767
ESR	0.267	0.580	0.095	0.070	0.136	0.246	0.063	0.027	0.543	0.843	0.088	0.271
ADMax	3.558	3.533	3.799	3.898	3.835	4.176	3.844	4.317	3.405	3.482	3.748	3.806
Tick	**0.092**	**0.092**	**0.092**	**0.092**	**0.092**	**0.092**	**0.092**	**0.092**	**0.093**	**0.092**	0.093	**0.092**
FZL	**1.222**	**1.221**	**1.226**	**1.222**	**1.226**	**1.235**	1.236	**1.231**	**1.227**	**1.224**	1.235	**1.226**
Panel B: Confidence level 99%												
mVaR	−3.571	−3.597	−3.438	−3.474	v3.488	−3.493	−3.400	−3.392	−3.670	−3.689	−3.481	−3.565
stdVaR	1.672	1.768	1.674	1.695	1.754	1.866	1.816	1.817	1.789	1.848	1.771	1.812
mES	−4.085	−4.472	−3.969	−4.139−	3.995	−4.309	−3.890	−4.036	−4.199	−4.642	−3.953	−4.266
stdES	1.913	2.322	1.988	2.132	2.008	2.450	2.155	2.297	2.047	2.432	2.074	2.283
AE	1.139	1.111	1.437	1.247	1.382	1.355	1.491	1.437	1.139	1.111	1.464	1.274
LR_{uc}	0.408	0.504	0.012	0.147	0.027	0.040	0.005	0.012	0.408	0.504	0.008	0.109
LR_{cc}	0.569	0.505	0.020	0.195	0.083	0.061	0.009	0.020	0.569	0.505	0.029	0.150
DQ	0.695	0.759	0.037	0.375	0.166	0.123	0.014	0.058	0.695	0.759	0.039	0.299
ER	0.003	0.929	0.038	0.281	0.014	0.730	0.006	0.195	0.039	0.993	0.047	0.550
ESR	0.080	0.644	0.046	0.138	0.079	0.397	0.049	0.052	0.214	0.830	0.053	0.388
ADMax	2.802	2.693	2.860	2.756	2.990	3.256	3.267	3.596	2.620	2.499	2.847	2.618
Tick	**0.044**	**0.043**	**0.044**	**0.043**	**0.044**	**0.044**	**0.044**	**0.044**	**0.044**	**0.043**	**0.044**	**0.043**
FZL	1.396	**1.380**	1.399	**1.382**	1.413	1.406	1.419	1.415	1.392	**1.376**	1.407	**1.382**

The table presents the mean values and standard deviations of VaR and ES forecasts at 97.5% (Panel A) and 99% (Panel B) confidence levels for short positions in PBD. Additionally, it includes backtesting outcomes for three GARCH variants paired with different distributions: normal (N), skewed *t* (ST), historical simulation (HS), or Cornish-Fisher expansion (CF), throughout the entire forecasting horizon. The table details the AE ratio, the *p*-values for the LR_{uc}, LR_{cc}, DQ, one-sided ER, one-sided Intercept ESR tests, alongside the absolute maximum deviation (ADMax) and mean values of the tick and FZL metrics. Models highlighted in bold denote those included in the superior set of models, which have statistically comparable VaR forecasts based on either the tick loss function or joint VaR and ES forecasts based on the FZL function at a 90% confidence level.

Table 11 ES99 vs VaR99 ratio.

	GARCH				GJRGARCH				IGARCH			
	N	**ST**	**HS**	**CF**	**N**	**ST**	**HS**	**CF**	**N**	**ST**	**HS**	**CF**
Panel A: PBW												
Long												
Full period	1.146	1.222	1.179	1.194	1.145	1.220	1.181	1.191	1.146	1.235	1.187	1.199
Sample I	1.157	1.228	1.377	1.235	1.158	1.228	1.391	1.238	1.155	1.248	1.312	1.249
Sample II	1.159	1.422	1.350	1.314	1.163	1.432	1.380	1.318	1.158	1.424	1.340	1.313
Sample III	1.159	1.403	1.396	1.314	1.158	1.404	1.486	1.315	1.159	1.405	1.413	1.314
Short												
Full period	1.145	1.197	1.156	1.160	1.146	1.193	1.167	1.162	1.145	1.208	1.149	1.163
Sample I	1.153	1.208	1.178	1.189	1.154	1.206	1.190	1.191	1.153	1.226	1.247	1.210
Sample II	1.157	1.366	1.207	1.267	1.157	1.370	1.236	1.271	1.156	1.368	1.212	1.266
Sample III	1.144	1.332	1.197	1.266	1.145	1.698	1.255	1.268	1.144	1.334	1.173	1.266
Panel B: PBD												
Long												
Full period	1.148	1.267	1.178	1.227	1.146	1.254	1.172	1.220	1.148	1.285	1.199	1.233
Sample I	na	na	na	na	na	na	na	na	na	na	na	na
Sample II	1.161	1.469	1.330	1.388	1.162	1.473	1.342	1.390	1.161	1.471	1.346	1.388
Sample III	1.168	1.459	1.554	1.530	1.172	1.459	1.676	1.537	1.168	1.470	1.624	1.559
Short												
Full period	1.144	1.234	1.151	1.184	1.145	1.222	1.138	1.180	1.144	1.250	1.130	1.189
Sample I	na	na	na	na	na	na	na	na	na	na	na	na
Sample II	1.149	1.414	1.354	1.350	1.152	1.417	1.301	1.354	1.148	1.416	1.268	1.351
Sample III	1.150	1.403	1.276	1.646	1.151	1.418	1.275	1.658	1.150	1.413	1.259	1.716

The table presents the ratio of ES (99% confidence) to VaR (99% confidence) forecasts for both long and short positions in PBW (Panel A) and PBD (Panel B). These comparisons are made across three GARCH-based models, each paired with either a normal distribution (N), skewed t distribution (ST), historical simulation (HS), or Cornish-Fisher expansion (CF). The table reports the average of these ratios over the entire forecast period, as well as the maximum ratio values observed over the sub-sample periods.

analysis of the one-day-ahead VaR forecasts at 99% confidence across the out-of-sample forecast period. Most notably, the GARCH with normal innovation (GARCH-Normal) model presented in the top row (Panels A and B) is visually the poorest performer across both indices. The dense clustering of red violation dots indicates that this baseline model systematically underestimates risk for both long and short positions, particularly during periods of high market volatility, underscoring the inadequacy of assuming normal distributions when modeling extreme risk events in the volatile clean energy sector.

A detailed examination of model performance by position type reveals distinct patterns. For long positions (left column, Panels A, C, E), the GJRGARCH with skewed-*t* innovation model (Panel C) demonstrates visibly superior performance, with its VaR forecast

Table 12 ES97.5 vs VaR99 ratio.

	GARCH				GJRGARCH				FIGARCH			
	N	ST	HS	CF	N	ST	HS	CF	N	ST	HS	CF
Panel A: PBW												
Long												
Full period	1.005	1.020	1.024	1.003	1.005	1.020	1.030	1.003	1.005	1.023	1.033	1.004
Sample I	1.005	1.020	1.130	1.008	1.005	1.020	1.153	1.008	1.005	1.025	1.108	1.011
Sample II	1.005	1.070	1.127	1.021	1.006	1.074	1.137	1.022	1.005	1.070	1.121	1.021
Sample III	1.005	1.064	1.137	1.022	1.005	1.064	1.183	1.022	1.005	1.064	1.135	1.022
Short												
Full period	1.005	1.017	1.018	0.999	1.005	1.014	1.023	1.000	1.005	1.020	1.011	1.000
Sample I	1.005	1.018	1.040	1.004	1.005	1.018	1.048	1.004	1.005	1.023	1.083	1.008
Sample II	1.005	1.060	1.027	1.019	1.005	1.061	1.036	1.020	1.005	1.060	1.049	1.019
Sample III	1.005	1.052	1.076	1.019	1.005	1.292	1.096	1.019	1.005	1.053	1.058	1.019
Panel B: PBD												
Long												
Full period	1.005	1.031	1.021	1.008	1.005	1.028	1.017	1.007	1.005	1.036	1.034	1.009
Sample I	na	na	na	na	na	na	na	na	na	na	na	na
Sample II	1.005	1.085	1.094	1.033	1.005	1.086	1.118	1.033	1.005	1.085	1.111	1.033
Sample III	1.006	1.082	1.190	1.058	1.006	1.082	1.280	1.059	1.006	1.085	1.192	1.062
Short												
Full period	1.005	1.027	1.019	1.004	1.005	1.023	1.013	1.003	1.005	1.031	1.001	1.005
Sample I	na	na	na	na	na	na	na	na	na	na	na	na
Sample II	1.005	1.074	1.121	1.034	1.005	1.075	1.068	1.034	1.005	1.075	1.079	1.034
Sample III	1.005	1.072	1.086	1.083	1.005	1.073	1.084	1.085	1.005	1.074	1.067	1.096

The table presents the ratio of ES (97.5% confidence) to VaR (99% confidence) forecasts for both long and short positions in PBW (Panel A) and PBD (Panel B). These comparisons are made across three GARCH-based models, each paired with either a normal distribution (N), skewed tt distribution (ST), historical simulation (HS), or Cornish-Fisher expansion (CF). The table reports the average of these ratios over the entire forecast period, as well as the maximum ratio values observed over the sub-sample periods.

line (in blue) being more adaptive to changes in market volatility,capturing the asymmetric response to negative shocks and resulting in noticeably fewer violation dots compared to the GARCH-Normal model. Conversely, for short positions (right column, Panels B, D, F), the IGARCH with skewed *t* innovation model (Panel F) emerges as the most effective specification, with its VaR forecast line (in purple) providing more appropriate risk boundaries for the upside return spikes characteristic of short-selling risk, leading to the fewest violations across both indices. These visual findings confirm that the optimal model for managing downside risk in long positions (GJRGARCH-st) differs from the optimal model for managing upside risk in short positions (IGARCH-st), thereby validating the necessity of a tailored, dual-model approach for comprehensive risk management in clean energy investments.

Discussion. This study offers valuable insights into risk forecasting for the volatile clean energy stock market, with findings that both reinforce and extend key themes from the broader VaR literature. The key results demonstrating the necessity of non-normal innovations and the divergent model requirements for long and short positions provide a clear pathway toward improving the predictive accuracy of VaR and ES for clean energy sector stocks, which is critical for both investors and regulators.

First, our study finds that non-normal innovations, specifically the skewed *t* distribution, outperform standard methods such as filtered historical simulation and the Cornish-Fisher expansion. The skewed *t* distribution excels at capturing both skewness and kurtosis, which is particularly important in the clean energy sector, where returns frequently exhibit asymmetric behavior and fat tails. This characteristic stems primarily from the sector's heightened sensitivity to rapid technical improvements and legislative shifts. By offering a more flexible and robust estimation approach, especially for the smaller sample sizes common in emerging markets, this distribution enhances the reliability of risk forecasts. The result aligns with a significant stream of literature emphasizing the importance of accounting for skewness in VaR forecasting of equity indices (Abad et al., 2016; Chen et al., 2012; Kuang, 2021). By demonstrating the superiority of the skewed *t*-distribution for clean energy assets, a sector defined by high uncertainty and frequent policy-driven shocks, our study validates these general findings within a new and economically significant domain.

Second, the disparity in optimal models for long and short positions represents this study's primary contribution to the literature on forecast improvement. While the challenge of producing reliable VaR forecasts during market stress has led researchers to explore various enhancement strategies, such as data-driven forecast combination techniques (Chiu et al., 2010; Halbleib and Pohlmeier, 2012), our research introduces a complementary perspective: forecast improvement through ex-ante model tailoring. This disparity can be attributed to the sector's asymmetric price dynamics and risk characteristics. For long positions, the GJRGARCH model outperforms due to its ability to capture the leverage effect, whereby negative shocks have a greater influence on volatility than positive shocks of equivalent magnitude. This is especially important in the renewable energy sector, where adverse developments, such as regulatory rollbacks, can substantially impact investor sentiment. In contrast, the IGARCH model is more successful for short positions, reflecting the persistent nature of volatility during upward trends, which are frequently driven by positive technology breakthroughs or supportive policy announcements. These findings suggest that a single, universally optimal model may not exist even within a specific asset class, and that tailoring models to the directional nature of risk exposure represents a crucial yet underexplored avenue for enhancing forecast accuracy.

Finally, the variability in VaR and ES projections underscores the dynamic nature of the clean energy stock market, characterized by pronounced volatility responses to global economic

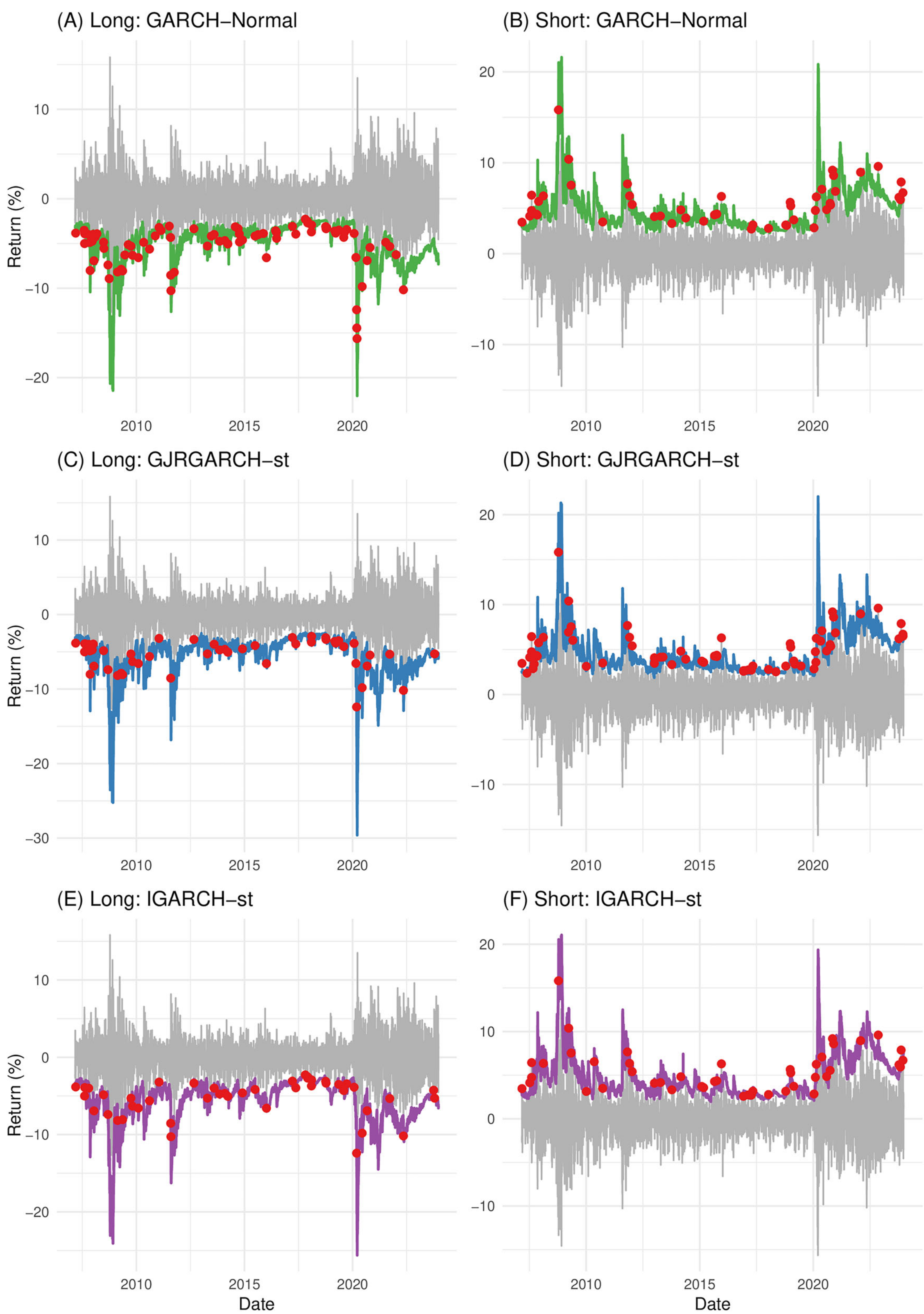

Fig. 3 Comparison of 99% VaR Forecasts for the PBW Index. The figure displays daily realized returns (grey line) against 99% VaR forecasts from three different models. The left column (**A**, **C**, **E**) shows the performance for a long position. The right column (**B**, **D**, **F**) shows the performance for a short position. Each row corresponds to a different model: GARCH-Normal (top), GJRGARCH-st (middle), and IGARCH-st (bottom). VaR violations, where losses exceeded the VaR estimate, are marked with red dots.

Fig. 4 Comparison of 99% VaR Forecasts for the PBD Index. The figure displays daily realized returns (grey line) against 99% VaR forecasts from three different models. The left column (**A**, **C**, **E**) shows the performance for a long position. The right column (**B**, **D**, **F**) shows the performance for a short position. Each row corresponds to a different model: GARCH-Normal (top), GJRGARCH-st (middle), and IGARCH-st (bottom). VaR violations, where losses exceeded the VaR estimate, are marked with red dots.

disruptions, technological developments, and policy changes (Attarzadeh and Balcilar, 2022; Zhang et al., 2023). As investor sentiment, technological progress, and macroeconomic factors evolve, risk managers must remain adaptable to shifting risk profiles. Our research demonstrates that employing both ES and VaR, consistent with the Basel regulatory shift toward Expected Shortfall for capturing tail risks (Taylor, 2020), facilitates a more comprehensive assessment of tail risks. This dual approach proves crucial for regulatory authorities seeking to refine capital adequacy requirements and risk management guidelines. These findings highlight the necessity for regulatory frameworks to be responsive to the distinct volatility characteristics and systemic risks inherent in clean energy investments. As the sector expands, continued risk model research and adaption will be critical for ensuring financial stability and supporting the industry's long-term development goals, particularly given the complex interplay between climate risks and financial stability considerations (Dietz et al., 2016).

Conclusion

This study contributes to the understanding of risk dynamics in clean energy investments by addressing the persistent challenge of tail risk modeling. By conducting a comprehensive empirical analysis focused on the unique characteristics of clean energy stocks, we demonstrate that a tailored, dual-model approach is essential for accurate risk management. Our key findings show that the GJRGARCH-skewed *t* model is best suited to long positions, whilst the IGARCH-skewed *t* model shines at short positions.

These findings have significant and actionable implications for risk management and portfolio optimization in the clean energy sector. For portfolio and risk managers, the practical benefits are multifaceted. First, adopting superior model specifications like the GJRGARCH-st for long positions leads to more accurate VaR and ES forecasts. This enhanced accuracy enables more efficient capital allocation, ensuring that capital reserves set aside to cover potential losses are neither inadequate (exposing the firm to unexpected risk) nor excessive (constraining profitable investment opportunities). The improved forecasting precision can translate into substantial cost savings, as financial institutions typically hold billions in regulatory capital that could be more productively deployed if risk estimates were more accurate.

Second, the daily risk forecasts from these dynamic models enable more responsive and proactive risk management strategies. For instance, a spike in forecasted VaR could trigger tactical position reductions, dynamic hedging adjustments, or the implementation of protective derivatives strategies, allowing investors to preemptively mitigate risk exposure in response to evolving market conditions. This real-time risk monitoring capability is particularly valuable in the clean energy sector, where regulatory announcements, technological breakthroughs, or policy shifts can rapidly alter risk profiles.

Furthermore, these models significantly enhance portfolio optimization decisions across multiple dimensions. By providing more accurate measures of volatility and tail risk-critical inputs for risk-adjusted performance metrics such as the Sharpe ratio, modified Sharpe ratio, and Sortino ratio, investors can make better-informed strategic asset allocation decisions regarding clean energy exposure. This improved risk measurement also facilitates more sophisticated portfolio construction techniques, such as risk parity strategies or maximum diversification approaches, which rely heavily on accurate volatility estimates.

From a regulatory and systemic risk perspective, our results underscore the inadequacy of standardized, one-size-fits-all risk models in capturing the nuanced risk characteristics of emerging sectors. The empirical finding that long and short positions require fundamentally different modeling approaches supports the ongoing regulatory shift towards more sophisticated internal models for calculating capital requirements under Basel and similar frameworks. As sustainable investments become increasingly integral to the global financial system, accurate risk measurement in clean energy assets becomes crucial not only for individual firm stability but also for broader financial system resilience and the successful transition to a sustainable economy.

Despite these contributions, our study has limitations. First, our analysis focuses on a small number of renewable energy indices, which may limit the generalizability of our findings. Future research should look at a broader range of clean energy assets, such as individual equities and sub-industry indexes, to validate and expand on our findings. Second, our study evaluated several competing parametric and non-parametric distributions for the innovations within the GARCH framework. A further refinement could be achieved by employing Extreme Value Theory (EVT) (McNeil and Frey, 2000), a specialized approach designed to directly model the extreme tails of the standardized residuals. While powerful, the application of EVT requires a very long time series to ensure the reliable estimation of tail parameters. As more historical data becomes available, integrating EVT to model the innovations' tails would be a valuable and logical extension of our work. Third, while our focus on GARCH-type models yields valuable insights, investigating alternative methodology, such as machine learning approaches, could improve risk forecasting in this dynamic sector. Finally, the study's reliance on historical backtesting may fail to adequately account for future market changes caused by regulatory reforms or unexpected economic upheavals. Integrating scenario analysis or stress testing could be beneficial in future investigations.

In conclusion, the insights from this research are both timely and relevant as the world moves towards sustainable energy investments. By refining traditional risk models to better encapsulate the complexities of clean energy stocks, we offer a more precise and adaptable framework for risk assessment in this critical sector. As clean energy markets expand, our findings will help to guide investment decisions, strengthen financial resilience, and contribute to the overarching aims of sustainable development.

Data availability

The datasets generated and analyzed during the current study are available in the Harvard Dataverse repository (https://doi.org/10.7910/DVN/KKVLJK). Source data were originally retrieved from investing.com.

Received: 8 October 2024; Accepted: 31 October 2025;
Published online: 17 December 2025

References

Abad P, Benito S, Martín CL (2016) Evaluating the performance of the skewed distributions to forecast value-at-risk in the global financial crisis. J Risk 18:1–28

Ahmad W, Sadorsky P, Sharma A (2018) Optimal hedge ratios for clean energy equities. Econ Model 72:278–295

Alessi, L., Savona, R. Machine learning for financial stability. *Data Science for Economics and Finance: Methodologies and Applications*. Cham: Springer International Publishing; 65-87 (2021)

Angelidis T, Degiannakis S (2005) Modeling risk for long and short trading positions. J Risk Financ 6(3):226–238

Athari SA, Kirikkaleli D (2025) How do climate policy uncertainty and renewable energy and clean technology stock prices co-move? evidence from Canada. Empir Econ 68:353–371

Attarzadeh A, Balcilar M (2022) On the dynamic connectedness of the stock, oil, clean energy, and technology markets. Energies 15:1893

Baillie RT, Bollerslev T, Mikkelsen HO (1996) Fractionally integrated generalized autoregressive conditional heteroskedasticity. J Econ 74(1):3–30

Barone-Adesi G, Giannopoulos K, Vosper L (1999) VaR without correlations for portfolios of derivative securities. J Futures Mark 19(5):583–602

Bayer S, Dimitriadis T (2022) Regression-Based Expected Shortfall Backtesting. J Financ Econom 20(3):437–471. https://doi.org/10.1093/jjfinec/nbaa013

BCBS. Minimum capital requirements for market risk. (2016) *Basel Committee on Banking Supervision*

Berger T, Missong M (2014) Financial crisis, value-at-risk forecasts and the puzzle of dependency modeling. Int Rev Financial Anal 33:33–8

Black, F. Studies of stock price volatility changes. *Proceedings from the American statistical association, business and economic statistics section*. (1976)

BloombergNEF. Energy Transition Investment Trends 2024. https://assets.bbhub.io/professional/sites/24/Energy-Transition-Investment-Trends-2024.pdf. Published: January 30, (2024)

Bollerslev T (1986) Generalized Autoregressive Conditional Heteroskedasticity. J Econ 31:307–27

Bollerslev T, Wooldridge JM (1992) Quasi-maximum likelihood estimation and inference in dynamic models with time-varying covariances. Econom Rev 11:143–72

Brio EBD, Mora-Valencia A, Perote J (2020) Risk quantification for commodity ETFs: Backtesting value-at-risk and expected shortfall. Int Rev Financial Anal 70:101163

Chen Q, Gerlach R, Lu Z (2012) Bayesian Value-at-Risk and expected shortfall forecasting via the asymmetric Laplace distribution. Comput Stat Data Anal 56:3498–516

Chen J, Liang Z, Ding Q, Liu Z (2022) Extreme spillovers among fossil energy, clean energy, and metals markets: Evidence from a quantile-based analysis. Energy Econ 107:105880

Chiu Y-C, Chuang I-Y, Lai J-Y (2010) The performance of composite forecast models of value-at-risk in the energy market. Energy Econ 32:423–31

Christoffersen PF (1998) Evaluating Interval Forecasts. Int Economic Rev 39:841–62

Christoffersen, P.F. (2012) Elements of Financial Risk Management (2nd ed.). Academic Press

Demiralay S, Gencer G, Kilincarslan E (2023) Risk-return profile of environmentally friendly assets: Evidence from the NASDAQ OMX green economy index family. J Environ Manag 337:117683

Di Febo E, Foglia M, Angelini E (2021) Tail risk and extreme events: connections between oil and clean energy. Risks 9(2):39

Dietz S, Bowen A, Dixon C, Gradwell P (2016) Climate value at risk of global financial assets. Nat Clim Change 6:676–9

Dutta A, Bouri E, Saeed T, Vom XV (2020) Impact of energy sector volatility on clean energy assets. Energy 212:118657

Efron B, Tibshirani RJ (1993) An Introduction to the Bootstrap. Chapman and Hall, New York

Engle RF (1982) Autoregressive Conditional Heteroscedasticity with Estimates of the Variance of United Kingdom Inflation. Econometrica 50(4):987–1007

Engle RF, Bollerslev T (1986) Modelling the persistence of conditional variances. Econom Rev 5(1):1–50

Engle RF, Ng VK (1993) Measuring and testing the impact of news on volatility. J Financ 48(5):1749–1778

Engle RF, Manganelli S (2004) CAViaR. J Bus Economic Stat 22(4):367–81

Favre L, Galeano JA (2002) Mean-Modified Value-at-Risk Optimization with Hedge Funds. J Alternative Invest 5(2):21–5

Fernandez C, Steel MFJ (1998) On Bayesian Modeling of Fat Tails and Skewness. J Am Stat Assoc 93(441):359–71

Fissler T, Ziegel JF (2016) Higher order elicitability and osband's principle. Ann Stat 44(4):1680–707

Francq, C. and Zakoian, J.-M. (2019) GARCH models: structure, statistical inference and financial applications. *John Wiley & Sons*

Fu Z, Chen Z, Sharif A, Razi U (2022) The role of financial stress, oil, gold and natural gas prices on clean energy stocks: Global evidence from extreme quantile approach. Resour Policy 78:102860

Ghosh B, Papathanasiou S, Dar V, Kenourgios D (2022) Deconstruction of the green bubble during COVID-19: International evidence. Sustainability 14(6):3466

Glosten LR, Jagannathan R, Runkle DE (1993) On the Relation between the Expected Value and the Volatility of the Nominal Excess Return on Stocks. J Financ 48(5):1779–801

Gustafsson R, Dutta A, Bouri E (2022) Are energy metals hedges or safe havens for clean energy stock returns? Energy 244:122708

Halbleib R, Pohlmeier W (2012) Improving the value at risk forecasts: Theory and evidence from the financial crisis. J Economic Dyn Control 36:1212–28

Hamilton, J.D. (2020) Time series analysis Princeton University Press

Hansen PR, Lunde A, Nason JM (2011) The Model Confidence Set. Econometrica 79(2):453–97

Hassan A (2023) External energy security elements and the riskiness of clean energy stocks: a volatility analysis. Sustainability Account, Manag Policy J 14(2):396–419

Henriques I, Sadorsky P (2008) Oil prices and the stock prices of alternative energy companies. Energy Econ 30(3):998–1010

International Energy Agency. Renewables 2023 Analysis and forecast to 2028. https://iea.blob.core.windows.net/assets/96d66a8b-d502-476b-ba94-54ffda84cf72/Renewables_2023.pdf. Published: January, (2024)

International Energy Agency. Renewables 2024 Analysis and forecast to 2030. https://iea.blob.core.windows.net/assets/17033b62-07a5-4144-8dd0-651cdb6caa24/Renewables2024.pdf. Published: October, (2024)

Inchauspe J, Ripple RD, Truck S (2015) The dynamics of returns on renewable energy companies: A state-space approach. Energy Econ 48:325–35

Kuang W (2021) Dynamic VaR forecasts using conditional Pearson type IV distribution. J Forecast 40(3):500–11

Kuang W (2022) Oil tail-risk forecasts: from financial crisis to COVID-19. Risk Manag 24(4):420–60

Kumar S, Managi S, Matsuda A (2012) Stock prices of clean energy firms, oil and carbon markets: A vector autoregressive analysis. Energy Econ 34(1):215–226

Kupiec PH (1995) Techniques for Verifying the Accuracy of Risk Measurement Models. J Derivatives 3:73–84

Lambert P, Laurent S. (2001) Modelling financial time series using GARCH-type models with a skewed student distribution for the innovations. *Mimeo: University of Liege*; 0125

Lehnert T (2023) The green stock market bubble. Circular Econ Sustainability 3(3):1213–22

Li B (2023) The role of financial markets in the energy transition: an analysis of investment trends and opportunities in renewable energy and clean technology. Environ Sci Pollut Res 30(43):97948–97964

Liu T, Nakajima T, Hamori S (2022) The impact of economic uncertainty caused by COVID-19 on renewable energy stocks. Empir Econ 62(4):1495–1515

Louzis DP, Xanthopoulos-Sisinis S, Refenes AP (2014) Realized volatility models and alternative Value-at-Risk prediction strategies. Economic Model 40:101–16

Managi S, Okimoto T (2013) Does the price of oil interact with clean energy prices in the stock market? Jpn World Econ 27:1–9

McAleer M, Medeiros MC (2008) Realized Volatility: A Review. Econom Rev 27(1-3):10–45

McNeil AJ, Frey R (2000) Estimation of tail-related risk measures for heteroscedastic financial time series: an extreme value approach. J Empir Financ 7(3):271–300

Naeem MA, Arfaoui N (2023) Exploring downside risk dependence across energy markets: Electricity, conventional energy, carbon, and clean energy during episodes of market crises. Energy Econ 127:107082

NS Energy. US investor confidence in renewables and energy storage hits all-time high. https://www.nsenergybusiness.com/industry-news/us-investor-confidence-renewables/. Published: June 15 (2021)

Ortas E, Moneva JM (2013) The Clean Techs equity indexes at stake: Risk and return dynamics analysis. Energy 57:259–69

Patra S (2021) Revisiting value-at-risk and expected shortfall in oil markets under structural breaks: The role of fat-tailed distributions. Energy Econ 101:105452

Patton AJ (2011) Volatility forecast comparison using imperfect volatility proxies. J Econ 160(1):246–56

Pradhan AK, Tiwari AK (2021) Estimating the market risk of clean energy technologies companies using the expected shortfall approach. Renew Energy 177:95–100

Reboredo JC, Rivera-Castro MA, Ugolini A (2017) Wavelet-based test of co-movement and causality between oil and renewable energy stock prices. Energy Econ 61:241–252

Rezec M, Scholtens B (2017) Financing Energy Transformation: The Role of Renewable Energy Equity Indices. Int J Green Energy 14:368–78

Sadorsky P (2012) Correlations and volatility spillovers between oil prices and the stock prices of clean energy and technology companies. Energy Econ 34(1):248–255

Sadorsky P (2012) Modeling renewable energy company risk. Energy Policy 40:39–48

Sadorsky P (2022) Using machine learning to predict clean energy stock prices: how important are market volatility and economic policy uncertainty? J Clim Financ 1:100002

Saeed T, Bouri E, Alsulami H (2021) Extreme return connectedness and its determinants between clean/green and dirty energy investments. Energy Econ 96:105017
Sheikh AZ, Qiao H (2010) Non-normality of market returns: A framework for asset allocation decision making. J Alternative Invest 12(3):8
Song Y, Ji Q, Du Y-J, Geng J-B (2019) The dynamic dependence of fossil energy, investor sentiment and renewable energy stock markets. Energy Econ 84:104564
Syuhada K, Hakim A, Suprijanto D (2024) Assessing systemic risk and connectedness among dirty and clean energy markets from the quantile and expectile perspectives. Energy Econ 129:107261
Tan X, Geng Y, Vivian A, Wang X (2021) Measuring risk spillovers between oil and clean energy stocks: Evidence from a systematic framework. Resour Policy 74:102406
Taylor JW (2020) Forecast combinations for value at risk and expected shortfall. Int J Forecast 36:428–41
Tran MH, Tran NM (2023) Value-at-risk and the global financial crisis. J Risk Model Valid 17:41–83
Troster, V., Shahbaz, M., Macedo, D.N. (2020) Optimal Forecast Models for Clean Energy Stock Returns. In: Econometrics of Green Energy Handbook: Economic and Technological Development. 89–109 (2020)
Wang W (2024) Machine Learning in Financial Time-series Data. Adv Econ, Manag Political Sci 92:293–299
WilderShares LLC. Q2 WilderHill Quarterly Report. https://wildershares.com/pdf/2022
WilderShares LLC. Q4 WilderHill Quarterly Report. https://wildershares.com/pdf/2022
Xia T, Ji Q, Zhang D, Han J (2019) Asymmetric and extreme influence of energy price changes on renewable energy stock performance. J Clean Prod 241:118338
Zhang L, Wang L, Peng L, Luo K (2023) Measuring the response of clean energy stock price volatility to extreme shocks. Renew Energy 206:1289–300
Zhang J, Chen X, Wei Y, Bai L (2023) Does the connectedness among fossil energy returns matter for renewable energy stock returns? Fresh insights from the Cross-Quantilogram analysis. Int Rev Financial Anal 88:102659
Zhang H, Zhang Y, Gao W, Li Y (2023) Extreme quantile spillovers and drivers among clean energy, electricity and energy metals markets. Int Rev Financial Anal 86:102474
Xiaoli Z, Ye F, Ming F, Zhanhu H (2018) Do environmental regulations undermine energy firm performance? An empirical analysis from China's stock market. Energy Res Soc Sci 40:220–231
Zhao X (2020) Do the stock returns of clean energy corporations respond to oil price shocks and policy uncertainty? J economic Struct 9(1):53
Zhuo J, Ren X, Duan K (2023) Modelling extreme risks for green bond and clean energy. Environ Sci Pollut Res 30:83702–83716

Acknowledgements
This work was supported by the Guangdong Province Ordinary University Characteristic Innovation Project (Grant No. 2024WTSCX076).

Author contributions
Wei Kuang is the sole author of this manuscript and was responsible for all aspects of the research. This includes conceptualization and design of the study, development of the methodology, data collection and curation, formal statistical analysis, software implementation, preparation of the original draft, subsequent revisions and editing, creation of figures and visualizations, and overall project administration.

Competing interests
The authors declare no competing interests.

Ethical approval
This article does not contain any studies with human participants performed by any of the authors.

Informed consent
This article does not contain any studies with human participants performed by any of the authors.

Additional information
Correspondence and requests for materials should be addressed to Wei Kuang.